The effect of cycling hypoxia on MCF-7 cancer stem cells and the impact of their microenvironment on angiogenesis using human umbilical vein endothelial cells (HUVECs) as a model

Fuad M Alhawarat[1], Hana M Hammad[1], Majd S. Hijjawi[2], Ahmad S Sharab[2], Duaa A Abuarqoub[1], Mohammad A Al Shhab[2], Malek A Zihlif[2]

Department of Biological Sciences, School of Science, The University of Jordan, Amman 11942, Jordan

Department of Pharmacology, School of Medicine, The University of Jordan, Amman 11942, Jordan

Corresponding author

Malek Zihlif

m.zihlif@ju.edu.jo

ABSTRACT

Background: Breast cancer is the most common type of cancer among females. Hypoxia mediates cancer hallmarks and results from reduced oxygen level due to irregularities in tumor vascularization or when the tumor size prevents oxygen diffusion and triggers angiogenesis to compensate for low oxygen. Cancer stem cells (CSCs) are a rare subpopulation, able to self-renew and to give rise to tumor-initiating cells. It is proposed that CSCs' secretions help to recruit endothelial cells via angiogenic factors to establish tumor vascularization. In the tumor microenvironment, the effect of hypoxia on CSCs and the impact of their secretions on triggering angiogenesis and tumor vascularization remain questionable. In this study, the (3D) CSCs derived from MCF-7 were directly exposed to repetitive long-term cycles of hypoxia to assess its effect on CSCs and then to evaluate the role of the hypoxic CSCs' (CSCs^{HYP}) secretions in angiogenesis using (HUVECs) as a model for tumor neovascularization response.

30   **Methods:** CSCs derived from MCF-7 cell-line were expanded under repetitive, strictly
31   optimized, long-term/continuous and intermittent hypoxic shots for almost four months to assess
32   hypoxic effect on CSCs, sorted based on CD44^{+}/CD24^{-} biomarkers. Hypoxic phenotype of
33   CSCs[HYP] was evaluated by assessing the acquired chemoresistance using MTT assay and elevated
34   stemness properties were assessed by flow cytometry. To evaluate the effect of the secretions from
35   CSCs[HYP] on angiogenesis, HUVECs were exposed to CSCs[HYP] conditioned-medium (CdM) -in which
36   CSCs had been previously grown - to mimic the tumor microenvironment and to assess the effect of the
37   secretions   from CSCs[HYP] on the HUVECs' capability of tube formation, migration and wound healing.
38   Additionally, co-culture of CSCs[HYP] with HUVECs was performed.

39   **Results:** CSCs[HYP] acquired higher chemoresistance, increased stemness properties and obtained
40   greater propagation, migration, and wound healing capacities, when compared to CSCs in
41   normoxic condition (CSCs[NOR]). HUVECs' tube formation and migration abilities were mediated
42   by hypoxic (CSCs) conditioned media (CdM).

43   **Discussion**: This study demonstrates that chemoresistant and migrational properties of CSCs are
44   enhanced under hypoxia to a certain extent. The microenvironment of CSCs[HYP] contributes to
45   tumor angiogenesis and migration. Hypoxia is a key player in tumor angiogenesis mediated by
46   CSCs.

INTRODUCTION

48   Cancer Stem Cells (CSCs) are subpopulation in the cancer tissue that slowly divide with an
49   ability to regenerate by uneven cell division (Huang & Rofstad 2017), contributing to cancer
50   relapse, invasiveness and thus higher cancer mortality (Peitzsch et al. 2017). CSCs have the same
51   intrinsic features as normal stem cell populations found throughout the body, including the
52   ability of self-renewal and differentiation (Batlle & Clevers 2017).
53   In most solid tumors, including breast carcinoma, hypoxia is a mutual hallmark that is proven to
54   associate with poor prognosis of cancer patients (Muz et al. 2015). Various stress-response
55   pathways that drive cancer cells toward a self-stabilizing and anti-apoptotic phenotype are
56   activated upon the exposure of cells to sub-physiologic concentrations of oxygen ($\leq 1\%$ O_2) or
57   hypoxia (Crowder et al. 2014). Hypoxia stabilizes the hypoxia-inducible factor-α (HIFα) proteins
58   that contribute to various pro-survival processes in cancer cells, such as angiogenesis, abnormal
59   proliferation and metabolic alterations (Bristow & Hill 2008; Kietzmann et al. 2016; Kong et al.
60   2014), and thus increases the expression of pro-survival factors that support radioresistance and
61   chemoresistance (Crowder et al. 2014; Senthebane et al. 2017). The exact signaling pathways by
62   which hypoxia activates its effects are complex and remain under investigation. Among well-
63   recognized mechanisms are elevated genomic instability and irregular cell division (Crowder et

64   al. 2014; Hammer et al. 2007), uncontrolled reactive oxygen species and redox mechanisms,
65   aerobic glycolysis metabolic shift (Denko 2008), and reduced expression caused by
66   proapoptotic-factors   (Gordan et al. 2008).
67   Cycling hypoxia determines the state of oxygen level and its dispersal in solid tumor tissues.
68   Dysfunctional heterogenic blood supply and tumor irregular vascularity in cancer cause oxygen
69   fluctuation for irregular periods with intermittent re-oxygenation intervals (Brurberg et al. 2004;
70   Muz et al. 2015). Acute hypoxia is an immediate brief exposure to a short-term hypoxic status
71   where the blood vessel occlusion lasts for at least few minutes and up to 72 hours (Chaplin et al.
72   1987; Muz et al. 2015). These changes in the bloodstream and the limited oxygen availability
73   result in chronic hypoxia, which is more apparent in large-sized tumors and energizes long-term
74   cellular changes (Eales et al. 2016). In experimental protocols, chronic hypoxic exposure is
75   obtained by incubating cells in hypoxia up to several weeks (Cassavaugh & Lounsbury 2011).
76   Indeed, clinical responses to cancer therapy are directly affected by both chronic and acute
77   hypoxic sections in solid tumors, inducing their growth, metastatic ability, and cell death
78   resistance (Al-Hajj et al. 2003).
79   Angiogenesis, which is defined as tumor neovascularization is essential for tumor development
80   and maintenance (Kaur et al. 2005; Zhao & Adjei 2015). It is also considered an important
81   cellular parameter of tumorigenesis (Wang et al. 2015). Elevated levels of vascular endothelial
82   growth factors (VEGFs) are expressed by endothelial cells involved in angiogenesis and bone
83   marrow-derived progenitor cells, and moreover, many types of human cancer cells can also
84   secrete VEGFs (Kerbel 2008). Evidence from different studies indicates that CSCs show greater
85   potential for tumor initiation, generation, and production of higher levels of VEGFs than the non-
86   stem cells in cancer population, thus exhibiting more potent proangiogenic capability (Ping &
87   Bian 2011; Wang et al. 2016). CSCs with elevated VEGF levels are typical example for the
88   significance of angiogenesis in tumor progression (Ojha et al. 2017).
89   In conclusion, CSCs' secretions help to recruit endothelial cells via angiogenic factors to
90   establish tumor vascularization. Moreover, hypoxia triggers angiogenesis in cancer tissues. The
91   studies that investigate the effect of long-term hypoxia on CSCs are extremely rare, so the cross-
92   talk between long-term hypoxia and its effect on CSCs and their role in angiogenesis remains
93   questionable. In this context, we hypothesized that repetitive exposure to cycles of
94   hypoxia/normoxia conditions may be a driving force that promotes a   highly resistant and
95   invasive CSCs subpopulation, and CSCs are proposed to generate higher levels of tumor
96   vascularization, due to induced angiogenesis, than regular cancer tissues.

97 Accordingly, the present study aims at investigating the effect of long-term hypoxia on CSCs
98 and the impact of hypoxic CSCs (CSCs^{HYP}) secretions on angiogenesis in the tumor
99 microenvironment. CSCs were derived from MCF7 cell-line and were expanded under repetitive
100 strictly optimized long-term and intermittent hypoxic shots to assess the effect of hypoxia on
101 them. Both intermittent and long-term hypoxia were directly applied for almost four months on
102 sorted and identified CSCs as (3D) mammospheres. Thereafter, to assess the impact of secretions
103 of CSCs^{HYP} on angiogenesis, we used the conditioned-medium (CdM) in which CSCs^{HYP} were
104 expanded and grown -as it comprises the CSC^{HYP} secretions- to treat HUVECs and then examine
105 their angiogenic ability.

MATERIALS AND METHODS

106
107
108 Workflow for the methodology adopted in this study is summarized in (**Figure 1).**
109

110 *Culture Conditions*
111 The breast cancer cell line (MCF-7) was purchased from the American Type Culture Collection
112 (ATCC, USA), and was expanded as a monolayer in vented 75cm^2 cell culture flasks (Membrane
113 Solutions, USA) using RPMI 1640 media (HyClone, USA). The media was supplemented with
114 heat-inactivated fetal bovine serum (FBS) 10% (v/v) (HyClone, USA), antibiotics (100μg/ml
115 streptomycin and 100U/ml penicillin) (HyClone, USA), and 1% 2mM L-glutamine (HyClone,
116 USA). The cells were incubated in a designated incubator (Nuaire, China) at (5% CO_2 at 37°C).
117 All cell culture procedures were performed in sterile conditions under a class II biological safety
118 cabinet (Heal-Force, China). All used materials and disposables were disinfected with ethanol
119 76% before use.
120

121 *Mammosphere Cultures*
122

123 To obtain CSCs from MCF-7 cell line and propagate them as mammospheres, MCF-7 cells were
124 expanded in complete growth media described above as a single-cell suspension in a standing
125 flask to enhance the growth of CSCs as they tend to grow in non-adherent conditions. Two days
126 later, remaining cells were collected by centrifugation, washed in phosphate buffer saline, and
127 seeded in 6 well ultra-low adherence plates (Corning, NY) at a density of 10,000 cells/well. Cells
128 were expanded in serum-free DMEM/F12 (Sigma-Aldrich) media, supplemented with 20 ng/mL
129 basic fibroblast growth factor (GIBCO, USA), 20 ng/mL epidermal growth factor (MPBio,
130 USA), 2% B27 (GIBCO, USA), 10 μg/mL insulin (MPBio, USA), 0.5μg/mL hydrocortisone

131 (Nacalai, Japan), 0.4% bovine serum albumin (Sigma, USA), and 2 mM L-Glutamine (Biowest
132 Co., France). This is called mammospheres culture media. Cells were preserved in a humidified
133 incubator at 37 °C, 5% CO_2. Every two days, fresh media (2 mL) were added to each well
134 (without removal of the old one). At day seven, primary mammosphere clusters were counted,
135 then collected and centrifuged to form a pellet. In order to obtain single cells, the pellet was
136 enzymatically disaggregated with trypsin and dispersed by passing through a 40 μm pore-size
137 filter (Millipore, Billerica, MA). Single cells of primary mammospheres were collected for
138 sorting, using beads technique and identified by flow cytometry (detailed below) before and after
139 sorting. Disaggregated cells were cultured in ultra-low adherence flask (Corning, NY) instead of
140 well plates to obtain secondary mammospheres. Then, the same procedure was applied again to
141 obtain tertiary and quaternary mammospheres.

142 To calculate the percentage of mammosphere forming efficiency (%MFE), the number of
143 mammospheres was divided by the number of seeded cells and multiplied by hundred.
144 Mammospheres were counted under 10x magnification of an inverted light microscope
145 (Olympus, USA). Twenty one (21) days after initial seeding in ultra-low attachment and serum-
146 free media, a sufficient mammospheres' population was established.

147

148 ***Cell Viability***
149 Cellular viability was evaluated using the trypan blue method. After de-attachment and good
150 homogenization of cells until there was a single-cell suspension, a sample was taken and diluted
151 in 1:1 ratio with trypan blue (Sigma-Aldrich, UK). Then 10uL of the diluted mixture was loaded
152 on a hemocytometer (Neubauer Double, Zuzi, Spain) and inspected under an inverted light
153 microscope (Olympus, USA). Cells with shiny white appearance were considered viable and
154 counted because their cell membrane was impermeable to trypan blue, while blue-colored cells
155 were disregarded. Hypoxic cells' viability was checked upon every other split and compared to
156 its normoxic counterparts to assess proliferation changes. While mammosphere cells were
157 enzymatically disaggregated into single-cells in order to observe viability (Cassavaugh &
158 Lounsbury 2011).

159

160 ***CSCs Sorting with Magnetic Beads***
161 CD44$^+$/CD24$^-$ are the expression biomarkers of interest in MCF-7 derived mammospheres. At
162 day seven of the initial culture of mammospheres in 6-well plate, CSCs enriched with
163 CD44$^+$/CD24$^-$ were sorted from MCF-7 mammospheres using MagCellect CD24$^-$/CD44$^+$ Breast
164 Cancer Stem Cell Isolation Kit (R&D System, Cat. MAGH111) according to their protocol.

165   Initially, CD24^{+} cells were labeled and removed magnetically. Then from the CD24^{−} population,

166   CD44^{+} cells were sorted magnetically using a biotinylated human CD44+ antibody and

167   streptavidin-conjugated magnetic beads as a positive selection model. The efficiency of sorting

168   was assessed by staining recovered cells with fluorochrome-conjugated anti-human CD44^{+} and

169   CD24^{-} antibodies. Isolated CD44 [+]/CD24^{-} cells were later identified via FACS analysis.

170

171   ***Exposure to Hypoxia***

172   To create hypoxic conditions, an anaerobic atmosphere generating system, AnaeroGen Compact

173   (Oxoid, UK) was used. The AnaeroGen system is used in microbiology area to create the low

174   oxygen conditions needed for the growth of anaerobic bacteria. Here, we adopted the AnaeroGen

175   system to induce hypoxia into CSCs. The system consists of a gas generatingsachets and tightly

176   sealable bags. The sachet reacts promptly upon contact with air and consumes oxygen thus

177   reducing oxygen concentration to less than 1% inside the bag. It has been confirmed in previous

178   studies by using biochemical and electronic testing that this technique reduces oxygen content in

179   plastic bag to below 1% within 30 minutes (Chenevier-Gobeaux et al. 2013; Mellor et al. 2005).

180   The vented ultra-low attachment 75 cm^2 tissue culture flasks were placed inside the plastic bags

181   and the sachets were placed inside then sealed. After 21 days of culturing the mammosphere

182   CSCs, they were divided into two groups and exposed to hypoxic conditions intermittently

183   (**INTR**.) or continuously (**CONT.**). CSCs in the intermittent group were exposed to 10, 20, 30 or

184   40 hypoxic shots for 8 hours 3 times a week, denoted as (**INTR.10, INTR.20, INTR.30,** and

185   **INTR.40**) respectively, while CSCs in the continuous group was exposed to 5, 10, or 15 hypoxic

186   shots for 72 hours once per week, denoted as (**CONT.5, CONT.10, and CONT.15**). Apart from

187   these optimized hypoxic shots, CSCs mammospheres were also incubated in normoxic

188   conditions as control (CSCs[NOR]), using the same culture media and conditions that were used for

189   expansion of mammospheres detailed above.

190

191   ***Flow Cytometry to Examine Enrichment of CSCs Mammosphere with CD44^{+}/CD24^{-} under***

192   ***Hypoxia/Normoxia***

193   Flow cytometry was used to identify and characterize CD44^{+}/CD24^{-} surface phenotype, which is

194   in direct proportion to stemness, and was performed for parental MCF-7 cells, un-sorted

195   mammospheres, sorted CSCs mammospheres three days after sorting, CSCs mammospheres

196   which were 21 days-old all under normoxic conditions and finally for CSCs[HYP] exposed to shots

197   of **INTR.20**, **INTR.40**, **CONT.5** and **CONT.15**. Mammospheres were dispersed to obtain

198   single-cell populations as described above. The CSCs' mammosphere pellet was washed in

199   phosphate-buffer saline (PBS) (HyClone, USA) with 2% bovine serum albumin and stained with

200   APC-anti-mouse CD24 and PE-anti-mouse CD44 antibodies (BD Pharmingen, CA). CSCs

201   mammospheres were incubated in ice for 30 minutes, washed twice with PBS and then fixed in

202   PBS containing paraformaldehyde. The flow cytometric analysis was performed on a BD

203   FACSCalibur system (BD Biosciences, CA), and the identification was performed with the BD

204   Cellquest software (BD Biosciences).

205

206   ***Cytotoxicity Evaluation Using MTT Assay***

207   To examine the chemoresistance of MCF-7 parental cells and their derived CSCs, both CSCs[NOR]

208   and CSCs[HYP], drug resistance towards doxorubicin was used as an indicator. A CellTiter Cell

209   Proliferation Assay Kit® (Promega, Madison, USA) was used. This assay includes 3-(4,5-

210   Dimethylthiazol-2-yl)-2,5-diphenyl tetrazolium bromide (MTT) which is a yellow tetrazole

211   reduced by viable cells to purple formazan. Consequently, surviving cells

213 after being exposed to multiple concentrations of doxorubicin can be quantified by
214 spectrophotometry. The MTT proliferation assay was performed on MCF-7 parental cells seeded
215 as a monolayer in an adherent 96-well plate. Moreover, CSCs^{HYP} were dissociated into single-
216 cells, filtered, counted then seeded at a 7×10^3 cells/well density in a 96-well plate and incubated
217 for 24 hours before treatment. Each concentration was tested in triplicate on CSCs exposed to
218 (**INTR.10, INTR.20, INTR.30, and INTR.40**) or exposed to (**CONT.5, CONT.10, and**
219 **CONT.15**). A control experiment was done for sorted and identified CSCs^{NOR} from
220 mammospheres cultured under normoxic conditions.
221 Incremental serial dilutions of doxorubicin concentrations from 0.01 μM to 200 μM were used.
222 After 72 hours of incubation, old media was aspirated, and 100 μl of fresh media was added to
223 each well. Then, 15μl of MTT reagent was added to each well and incubated for 4 hours.
224 Solubilization/stop solution was added to each well and incubated for an hour. Absorbancy was
225 read using an Elisa reader (Sunrise basic sciences, Austria) at 570 nm wavelength. The half
226 maximal inhibitory concentration (IC$_{50}$) was calculated using GraphPad PRISM®7.04 software
227 (GraphPad Software, Inc.).
228

229 ***Endothelial Cells Isolation from Umbilical Cords***
230 Human umbilical cords were obtained from two delivering females at the Jordan University
231 Hospital after getting the approval of their Institutional Review Board (IRB), decision number
232 98/2018 and approval number (67/2018/481) and both patients having signed an informed
233 consent before sample collection.
234 Enzyme digestion technique was used to isolate endothelial cells from the human umbilical cord.
235 Debris on the outer surface of the cord was wiped using antiseptic solution. Any clots formed
236 inside the vein were removed by slight squeezing. The umbilical vein was washed with RPMI
237 medium (HyClone, USA) containing 1% penicillin/streptomycin (HyClone, USA) to remove
238 excess blood and debris using 20 mL syringe inserted into the cord. Then, 0.1% of type I
239 collagenase (Sigma-Aldrich, USA) was put inside the vein where it was incubated for 20 minutes
240 at 37°C for digestion. Hereafter, the vein was washed with 20 mL RPMI media (HyClone, USA)
241 to stop collagenase proteolytic activity and was centrifuged at 1500 rpm for 5 min. The resultant
242 pellet was resuspended in 5 ml endothelial cell growth medium EGM-2 media (Lonza,
243 Walkersville, MD, USA) which consists of the endothelial cell basal media EBM-2 with 10%
244 FBS and other additives (including VEGF, bFGF- Fibroblast Growth Factor, EGF-Epidermal
245 Growth Factor, and IGF-Insulin Growth Factor). HUVECs were expanded on 0.2% gelatin-
246 coated T25 tissue culture flask and incubated overnight. Next day media was renewed to get rid
247 of cells debris. Only passages earlier than 6 of HUVECs were used in all experiments.

248

249 *Collection of Conditioned-Medium From Hypoxic/Normoxic CSCs*

250 In order to obtain the conditioned-medium (CdM), CSCs were seeded as single cells at a density

251 of 10,000 cells/cm^2 in an ultra-low adherence 75 cm^2 flasks with serum-free DMEM/F-12 and

252 with supplements (mammospheres culture media detailed above). CSCs mammospheres were

253 starved overnight by washing them twice with serum and supplement free DMEM/F-12 media,

254 then centrifuged at 300 rpm for 10 minutes. Finally, the media was renewed without serum and

255 without supplements for 8 hours for intermittent and 72 hours for the continuous hypoxic

256 condition. The resultant CdM from where CSCs grown under hypoxia or normoxia were

257 collected, centrifuged at 300 rpm for 10 min to remove cellular components and filtered through

258 0.2 μm pore-size filters (Millipore, Billerica, MA). CdM from flasks under normoxic conditions

259 were used as a control. Aliquots of the CdM were stored at -80°C before being used. CdM were

260 collected from eight sources, from CSCs^{NOR}, and from CSCs^{HYP} grown under the hypoxic shots

261 (**INTR.10, INTR.20, INTR.30, INTR.40, CONT.5, CONT.10,** or **CONT.15**) and were utilized

262 in successive experiments as discussed subsequently.

263

264 *Capillary-Like Tube Structure Formation Assay using CSCs' Mammospheres (CdM) on*

265 *HUVECs*

266 The effect of the factors secreted in the CdM obtained from CSCs^{HYP} and from CSCs^{NOR} on the

267 angiogenic ability of HUVECs was examined through the formation of capillary tube-like

268 structures by HUVECs, using the in vitro matrigel angiogenesis assay to mimic the

269 microenvironment of CSCs. To eliminate the impact of growth factors in Matrigel, reduced

270 growth factor Matrigel (BD Biosciences, USA) was used. HUVECs were incubated for 6 hours

271 in endothelial basal medium (EBM-2, Lonza) without serum and supplements for starvation.

272 Briefly, the Matrigel stored at -20°C was thawed in ice to prevent premature polymerization.

273 Aliquots of 50μl were plated into each well of pre-chilled 96-well culture plates and were left to

274 polymerize at 37°C for 2 hours. HUVECs were removed from confluent cultures by treatment

275 with Trypsin 0.05% (HyClone, USA). HUVECs were collected using serum-containing media to

276 stop trypsin effect, then counted, centrifuged and washed with phosphate buffer saline, then

277 resuspended with CdM obtained from the different hypoxic episodes, including intermittent shots

278 (**INTR.10**, **INTR.20**, **INTR.30**, **INTR.40**) and continuous shots (**CONT.5, CONT.10,**

279 **CONT.15**) of hypoxia and from its normoxic counterparts as a control in triplicates. HUVECs

280 were seeded at a density of 2×10^4 cells/well. For quantification of tube formation complex, three

281 primary variables were used to determine the magnitude of tube formation, average of total

282 length of the branched tube, the number of loops and covered area. These variables were

283 measured by Wimasis Image Analysis software.

284

285 ***VEGF Quantification By Enzyme-Linked Immunosorbent Assay***

286 The CdM that was collected as described above, was used for the determination of VEGF levels
287 secreted by CSC^{HYP} and CSC^{NOR} using the Enzyme-Linked Immunosorbent kit. Human VEGF
288 quantitative ELISA assay (R&D Systems, Minneapolis, MN) was performed according to
289 manufacturer's instructions. A quantity of 200ul of the CdM from different CSCs^{HYP} treatments
290 was tested.

291

292 ***Cell Migration Assay of HUVECs***

293

294 HUVECs ability to migrate under the treatment of the CdM was investigated using a Transwell
295 plate of 8 um pore-size chamber (Corning, USA). HUVECs were starved overnight using EBM-
296 2 media serum and supplement free for 6 hours, then seeded in the upper chamber (insert) of the
297 24 well plate at density of $5x10^4$ cells in 500 uL of EBM -2 media, each placed into lower wells
298 containing 750 ul of CdM obtained from (**INTR.10**, **INTR.20**, **INTR.30**, **INTR.40**) intermittent
299 hypoxic shots in addition to continuous hypoxic shots **(CONT.5, CONT.10, CONT.15)**. The
300 same procedure was applied to the control by using serum-free EBM-2 media in the lower well
301 instead of CdM. Then, cells were allowed to migrate for 8 hours, then 70% cold ethanol was
302 used for 10 minutes to fix the chambers. Membranes were stained with 0.5% (w/v) crystal violet
303 (Sigma-Aldrich, St. Louis, MO, USA) for 30 minutes and afterward washed carefully with water.
304 Cotton swabs were used to remove the cells that were not able to migrate to lower wells.
305 Solubilizing bound crystal violet in methanol 100% (wt./vol) was used to quantify the migrated
306 cells. Cells were inspected under an inverted light microscope (Olympus, USA) and
307 photographed at 4x magnification. Each sample was done in triplicate and three fields were
308 measured from each to calculate the migration.

309

310 ***Direct and Indirect Co-culture of HUVECs and CONT.5 CSCs Mammospheres***

311

312 A co-culture system has been used to better understand how CSCs^{HYP} regulate their
313 microenvironment and interact with HUVECs as a vascularization model for angiogenesis and
314 migration.

315 *Direct Co-culture:*

316 HUVECs were seeded on 0.1% gelatin (Sigma, USA) coated 6-well plate until 40% confluency
317 in EGM-2 media. From the CSCs^{HYP} subpopulation exposed to **CONT.5**, a single hypoxic CSC

318   was co-cultured in contact with HUVECs. The plates were incubated for few hours to allow

319   CSCs^{HYP} adhere to the wells already seeded with HUVECs. Media was changed to a 1:1 mixture

320   of EBM-2 and DMEM/F-12 free from serum and supplements and incubated for 72 hours.

321   *Indirect Co-culture:*

322   Transwell plates of 0.4 μm pore size chambers were seeded with HUVECs in lower wells after

323   coating them with 0.1% gelatin, while CSCs^{HYP} that were exposed to **CONT.5** were seeded in

324   the upper chamber as co-cultured in a 1:1 mixture of EBM-2 and DMEM/F-12 free from serum

325   and supplements.

326   Control HUVECs were cultured in EBM-2 without serum and without supplements in both the

327   direct and indirect experiments.

328

329   ***Wound Healing Assay for HUVECs***

330   In a 6-well plate, HUVECs at a density of 12×10^4 were seeded till confluency. Then they were

331   incubated for 6 hours in EBM-2 media without serum to prevent any external factors from

332   contributing to wound closure. After 6 hours, using a 200uL micropipette tip, a straight wound-

333   like scratch was made into the cells. Then cells were treated with CSCs^{HYP} CdM obtained from

334   **INTR.10**, **INTR.20**, **INTR.30**, **INTR.40**, **CONT.5**, **CONT.10** and **CONT.15** hypoxic shots in

335   which CSCs^{HYP} were grown, in addition to the control which was treated with CdM obtained

336   from CSCs^{NOR}. Cells were carefully washed using phosphate buffer saline (HyClone, USA),

337   before and after making the scratch. Wound healing was inspected under an inverted light

338   microscope (Olympus, USA) and photographed after 48 hours and at the beginning of the

339   experiment. The surface area of the wound could not be calculated by image analysis software

340   because control cells started to die after 16 hours.

341

342   ***Wound Healing Assay for Hypoxic CSCs***

343   In a 6-well plate coated with 1% gelatin, CSCs were seeded at a density of 8×10^4 and incubated

344   overnight, using DMEM/F-12 media without serum to prevent any external factors from

345   contributing to wound closure. The subpopulation of CSCs used was originally cultured under

346   intermittent or continuous hypoxic conditions; **INTR.10**, **INTR.20**, **INTR.30**, **INTR.40,**

347   **CONT.5**, **CONT.10**, and **CONT.15** in addition to the control **CSCs^{NOR}** originally grown under

348   normoxia. They were all used upon confluency before being seeded in a gelatin-coated 6-well

349   plate to allow CSCs adherence as a 2D monolayer for wound healing assay. Using a 200uL

350   micropipette tip, a straight wound-like scratch was made. Cells were washed using phosphate

351   buffer saline, before and after making the scratch, and then relevant media was used; DMEM/F-

352   12 without serum. Wound healing was photographed at the beginning of the experiment and after

353   36 hours. The surface area of the wound was measured by image analysis (ImageJ 1.4.3.67

354   Launcher Symmetry Software).

355

356   *Statistical Analysis*

357   Results were presented as a mean ± SD. Experiments were performed in triplicate with

358   comparable results unless indicated otherwise. An ANOVA test was used to compare the

359   differences between replicates which were considered significant at $p \leq 0.05$. GraphPad Prism

360   (version 7.04, San Diego, CA) was used for statistical analysis.

361

362

363   **RESULTS**

364

365   *(3D) Mammospheres Derived from MCF-7 cells*

366   Mammosphere culture has been widely used to enrich CSCs. Thereof, MCF-7 mammospheres

367   were cultured in ultra-low adherence plates and flasks, in serum-free media with supplements

368   and successfully formed rigid and compact (3D) structures within 3-7 days **(Figure 2)**. The

369   mammosphere multicellular spheroidal clumps became larger in size at day 7 compared to earlier

370   days of growth as shown in **(Figure 2)** with 30 um scale bar comparison. Moreover, as a

371   quantitative measure, at day seven the mammosphere formation efficiency (MFE) of MCF-7

372   cells was 0.012% (± 0.002%) only and after three weeks the MFE had increased to 5.30% (±

373   0.307%).

374

375   *Sorting of CSCs From 3D Mammospheres Using Magnetic Beads*

376   The magnetic beads separation protocol uses antibodies conjugated to a magnetic bead. CSCs

377   were successfully sorted and isolated using the magnetic beads technique, but their number

378   became sufficient only 3 days after sorting. Thereafter, sorted CSCs were identified via FACS

379   analysis and were used for hypoxic-condition exposure. The expression of $CD44^+/CD24^-$

380   mammospheres is shown in **(Table 1)** and their morphology is shown in **(Figure 2).**

381

382   *Enrichment of sorted CSCs mammospheres under Hypoxic/Normoxic Conditions*

383   The morphology of $CSCs^{HYP}$ and the control in normoxia $CSCs^{NOR}$ is shown in **(Figure 3)**. It is

384   observed that $CSCs^{HYP}$ that underwent **CONT.5** and **INTR.20** hypoxic shots were denser and

385   larger in number than $CSCs^{NOR}$. $CSCs^{HYP}$ that underwent **CONT.15** and **INTR.40,** that is the

386   maximum and final hypoxic shots showed the least growth compared to other hypoxic exposures

387   and $CSCs^{NOR}$. The MFE could not be measured for $CSCs^{HYP}$ because long-term hypoxic

388   exposure **(INTR.40** and **CONT.15)** made mammospheres aggregate into clumps, thus, the single

389 mammosphere could not be distinguished and compared to control and to other hypoxic
390 mammospheres.
391

Identification of CD44$^+$/CD24$^-$ Phenotype Content by Flow Cytometry

Flow cytometry conducted for CSCs after 3 days of sorting showed a percentage of CD44$^+$/CD24$^-$ expression equal to 81.0 ($\pm$ 7.5%). Three weeks (21 days) after growing in ultra-low attachment flasks, the percentage decreased to approximately 35.5 ($\pm$ 4.5%). In contrast, the parental MCF-7 cells had only 1 ($\pm$ 0.1%) expression and the unsorted mammospheres had 33.2 ($\pm$ 3%) expression. After exposure to hypoxic conditions, flow cytometry results based on CD44$^+$/CD24$^-$ markers showed that the highest expression occurred in CSCs^{HYP} exposed to **INTR.20** shots, 39.8 ($\pm$ 5.2%), and in CSCs^{HYP} exposed to **CONT.5,** 51.6 ($\pm$ 6.1%). On the other hand, the lowest percentages were observed in CSCs^{HYP} that underwent or were exposed to **INTR.40** shots, 0.3 ($\pm$ 0.01%), and in CSCs^{HYP} exposed to **CONT.15,** 0.5 ($\pm$ 0.05 %). In conclusion, isolated and sorted CD44$^+$/CD24$^-$ breast cancer cells only temporarily preserve this phenotype and ultimately revert to an equilibrium state in which the expanded sub-population regains the original cell surface profile of the parental cell line, which was deduced because the unsorted mammospheres and the 3-week old sorted CSCs both have similar CD44$^+$/CD24$^-$ content (33.2% and 35.5%, respectively). The CD44$^+$/CD24$^-$ percentage in unsorted mammospheres that were grown in ultra-low attachment plates in serum-free media for 7 days before sorting was 33.2 ($\pm$ 3%), which is much higher than the percentage of parental MCF-7 cells 1.0 ($\pm$ 0.1%). The expression of CD44$^+$/CD24$^-$ content for all subpopulations is summarized in (Table 1) and demonstrated in (Figure 4).

Hypoxic CSCs Show Higher Drug Resistance to Conventional Chemotherapies

To examine whether self-renewing CSCs mammospheres have higher chemoresistance ability, and to assess if hypoxic treatment of CSCs would increase their stemness character and chemoresistance, MTT assay was implemented to test the sensitivity of parental MCF-7 versus the sorted CSCs mammosphere towards doxorubicin. In addition, we assessed the resistance towards doxorubicin acquired by CSCs^{HYP} which underwent intermittent hypoxic shots **(INTR.10, INTR.20, INTR.30 INTR.40)**, and CSCs^{HYP} that underwent continuous hypoxic shots **(CONT.5, CONT.10, CONT.15)**. Then we compared the inhibitory drug concentration (IC$_{50}$) results for the CSCs^{HYP} versus CSCs^{NOR} mammospheres (as control) and compared the IC$_{50}$ value of CSCs^{HYP} versus parental MCF-7 cells, described in **Table 2**. Overall, the drug resistance of CSCs^{NOR} was found to be higher (IC$_{50}$=1.90 uM) when compared to the parental MCF-7 cells (IC$_{50}$=0.46 uM) by 4.08 times. Comparing the IC$_{50}$ values of CSCs^{NOR} mammospheres with CSCs^{HYP}, we observed significantly increased values under hypoxic conditions at **INTR.20** (IC$_{50}$=6.13 uM) and **CONT.5** (IC$_{50}$=7.12 uM) with (3.28) and (3.76) fold

426   increases respectively compared to IC_{50} of $CSCs^{NOR}$ mammospheres. These increaseswere much
427   higher upon comparing IC_{50} for $CSCs^{HYP}$ with parental MCF-7. The lowest IC_{50} values were
428   observed at **INTR.40** and **CONT.15** which represent the final hypoxic treatments. Taken
429   together, these results support the likelihood that enriching the mammospheres' culture with
430   CSCs contributed to the higher drug resistance toward doxorubicin when compared to the
431   parental MCF-7.
432
433   ***Hypoxic Conditioned Medium (CdM) Induces HUVECs to Form Capillary-Like Tube***
434   ***Structures in Matrigel***
435   In this study, HUVECs were treated with CdM in which CSCs were expanded under several
436   hypoxic and normoxic conditions, as described in the method section. Our results showed that
437   treating HUVECs with CdM obtained from $CSCs^{HYP}$ resulted in an increased construction of
438   capillary-like tube structures that reached its peak at 8 hours of treatment and disappeared
439   eventually in a time-dependent manner. However, HUVECs treated with CdM obtained from
440    $CSCs^{NOR}$ (control), resulted in a reduced formation of complex tubular structures compared to
441   the ones treated with the CdM obtained from $CSCs^{HYP}$ **(Figure 5)**. The capillary-like tube
442   structures were evaluated by quantitative analysis using Wimasis Image Analysis. The results
443   showed that the highest increase of branched tube lengths, the number of loops and the covered
444   area was with HUVECs that were cultured with CdM obtained from $CSCs^{HYP}$ culture that
445   underwent **INTR.20** and **CONT.5** shots at each time point (as demonstrated in Figures 5 and 6).
446   A bar graph (data combined from three independent trials) (Figure 6) shows that "the total length
447   of the tubes" underwent a remarkable increase upon the treatment with CdM from **INTR.20** and
448   **CONT.5,** by almost 2.4 fold in both **INTR.2**0 and **CONT.5** when compared to the control,
449   moreover, the "covered area" significantly increased when HUVECs were cultured with CdM
450   from $CSCs^{HYP}$ culture that underwent **CONT.5** and **INTR.20,** by 3.5 and 2.7 times respectively.
451   The total number of loops were significantly increased by 6.7 fold in **INTR.20** and 8.9 fold in
452   **CONT.5** compared to control HUVECs incubated with CdM obtained from the $CSCs^{NOR}$ culture
453   expanded in normoxic state. As shown in **(Figures 5 & 6)**, CdM induced a significant increase in
454   tube formation in HUVECs starting from the treatment with **INTR.10** CdM and reaching a
455   maximum at **INTR.20** (Figure 5F), whereas **CONT.5** (Figure 5B) caused the highest increase in
456   tube formation.
457
458   ***Detection of Secreted VEGF in Conditioned-Medium (CdM) by ELISA***
459   In order to identify the possible mediators of angiogenesis in breast cancer, a quantitative assay

460   was performed for the main angiogenic factor, VEGF-A. As the CdM obtained from the hypoxic

461   episodes **INTR.20**, **INTR.30** and **CONT.5** had the highest VEGF concentrations, **INTR.20,**

462   1159 (± 90 pg/ml), **INTR.30,** 1013 (± 32 pg/ml) and **CONT.5**, 934 (± 28 pg/ml) are compared to

463   control normoxic CdM 225 (± 24 pg/ml) as shown in **(Figure 7)**.

464

465   ***Effect of Conditioned-Medium (CdM) on Migration of HUVECs***

466

467   The role of the CdM in promoting migration of HUVECs was investigated using migration assay

468   to confirm whether secretions of CSCs^{HYP} enhance angiogenesis in the tumor microenvironment.

469   HUVECs were tested for their ability to migrate toward CdM from different hypoxic episodes

470   compared to their migration toward endothelial basal medium (EBM-2) serum and supplement

471   free, as a control, using transwell migration assay. The Transwell migration assay is used to

472   create a chemical gradient by putting the CdM in the lower chamber. Comparing the migration of

473   HUVECs from upper chamber across the membrane upon using the EBM-2 without serum and

474   without supplements (control) group versus using the CdM obtained from hypoxic shots, it was

475   found that migration was much higher under the use of the hypoxic CdM **(Figure 8)**. The assay

476   results showed that there were more purple-stained cells migrating toward the CdM obtained

477   from the **CONT.5** shot than the other two episodes (**CONT.10** and **CONT.15**). The CdM

478   obtained from the **INTR.20** episode had also more purple-stained cells migrating towards it,

479   compared to the other three episodes (**INTR.10**, **INTR.30,** and **INTR.40**). Interestingly, a

480   significant difference found was that the migrated-cell count in HUVECs towards CdM from

481   **CONT.5** vs control was 45000 (±2.1) *vs*. 4500 (±1.5), while the migrated cell count in **INTR.20**

482   vs control was 38000 (±2.6) *vs*. 4500 (±1.5). These findings suggest that the secretions presented

483   in the CdM which were obtained from **CONT.5** and **INTR.20** episodes significantly promoted

484   the migration of HUVECs. The data also showed that the migration capacity of HUVECs

485   increased significantly (10-fold) when cultured using the CdM from **CONT.5** shot and (8.4-fold)

486   when cultured using the CdM from **INTR.20** shot compared with HUVECs cultured with control

487   **(Figure 8).**

488

489   ***Stimulation of HUVECs Growth & Morphological Alterations in Co-Culture With   CSCs^{HYP}***

490   To clarify the interaction between endothelial cells and CSCs^{HYP} in the tumor microenvironment,

491   HUVECs were examined in direct and indirect co-cultures with the CSCs^{HYP} subpopulation that

492   underwent **CONT.5** episode. The control of HUVECs was cultured in serum and supplement

493   free media and possessed a 'teardrop-like' morphology. In the direct co-culture model, the

494   endothelial cell morphology changed and acquired elongated threadlike shape as a response to
495   the influence of CSCs^{HYP} secretions though the growth media was free from serum and any
496   growth factors as shown in (Figure 9. A, B, C).
497   We also examined the growth of HUVECs indirectly co-cultured with CSCs^{HYP} using a 0.4 uM
498   permeable membrane that was placed between HUVECs and CSCs^{HYP} subpopulation. Indirect
499   co-culture of the subpopulation of **CONT.5** CSCs^{HYP} with HUVECs induced sequential
500   morphological changes. As a response to the influence of secretions from CSCs^{HYP} thattrans-
501   passed through the membrane, the morphology of HUVECs began to change at 72 hours,
502   forming net-like structures resembling a vascular network, though the growth media was free
503   from serum and any growth factors (Figure 9-D & E). Control HUVECs proliferation reached a
504   plateau in 24 hours after which cells started to die.

505

506   ***In Vitro Wound-Healing Assay of HUVECs***
507   This assay was done to assess how secretions from CSCs^{HYP} in the tumor microenvironment
508   would affect the ability of HUVECs to migrate in response to chemoattractants in the CdM
509   obtained from different hypoxic shots. This model mimics the tumor microenvironment where
510   angiogenic ability of endothelial cells is affected by secretions from CSCs^{HYP}. In the control
511   experiment, HUVECs were treated with CdM obtained from CSCs^{NOR}. In the presence of the
512   CdM obtained from hypoxic shots, HUVECs were able to migrate and the wound closure was
513   enhanced after 48 hours. The wound closure was significantly enhanced by CdM obtained from
514   **INTR.20 (Figure 10-B)** and **CONT.5 (Figure 10-C)** shots. Whereas in the case of the control,
515   HUVECs that were treated with CdM media obtained from CSCs^{NOR}, showed a weaker capacity
516   to migrate. The wound surface area could not be calculated in order to assess wound closure
517   because the HUVECs treated with CdM obtained from CSCs^{NOR} and from CSCs^{HYP} after long-
518   term exposure (**INTR.40 and CONT.15)** started to die after 16 hours of treatment which
519   prevented further quantitative measurements.

520

521   ***In Vitro Wound-Healing Assay of Hypoxic CSCs***
522   Due to the significant role that CSCs play in tumor recurrence and metastasis, a wound-healing
523   assay was performed. CSCs were seeded as a (2D) monolayer, scratched, and then cell migration
524   was evaluated. The seeded CSCs were originally expanded and grown in hypoxic conditions,
525   **INTR.10**, **INTR.20**, **INTR.30, INTR.40**, **CONT.5**, **CONT.10,** and **CONT.15** in addition to the
526   control CSCs in normoxia. The scratched CSCs^{HYP} and CSCs^{NOR} cultured in DMEM/F-12
527   without serum were assessed for wound closure ability which was determined by calculating the

528 ratio of the wound surface area at the endpoint (36 hours) to its surface area at the starting point
529 of the experiment (zero hour). Images were analyzed by ImageJ software. Subpopulations of
530 CSCs^{HYP} showed greater ability for wound closure compared to CSCs^{NOR} (Figure 11-12).
531 CSCs^{HYP} from **INTR.20** and from **CONT.5** manifested the greatest wound closure (Figure 11).
532 At 36 hours, the wound closure of the control was only 40%, while it was 98% and 95% for
533 **INTR.20** (Figure 12-C) and **CONT.5** (Figure 12-F), respectively.
534
535 ## DISCUSSION

536 The initial stage of our study focused on the formation and characterization of MCF-7
537 mammospheres enriched with CSCs. The mammosphere culture is an approach to culturing
538 cancer cells in a three-dimensional (3D) conformation *in vitro*. These 3D models have been well
539 recognized in breast cancer research due to the great similarity of these models to the *in vivo*
540 solid tumors (Weiswald, Bellet et al. 2015, Boo, Ho et al. 2016). The 3D models are not only
541 biologically spherical in shape, but also possess many shared features with solid tumors which
542 were not observed in traditional 2D monolayer cultures (Baker and Chen 2012, Ekert, Johnson et
543 al. 2014). Interestingly, several current reports have shown that CSCs are particularly enriched
544 and maintained in cultures of 3D mammospheres (López, Poitevin et al. 2012, Liu, Ma et al.
545 2013). CSCs show a tendency to differentiate in the availability of serum, accordingly serum-
546 free culture conditions are believed to maintain the CSCs in an undifferentiated stage supporting
547 their enrichment, with recognizable loss and reduction in the size of the upper cell in the
548 hierarchical structure (Kruyt & Schuringa 2010; Lin et al. 2012). The results of our study have
549 shown a CD44+/CD24− expression **(Table 1)** for parental MCF-7 of (1%). After being cultured
550 in a low-adherence, serum-free, with supplements media, CSCs were sorted and again identified
551 with (FACS) and showed an extreme elevation of CD44+/CD24− expression to (81.3%) only
552 three days after being grown in mammosphere culture conditions, while it was (33.2%) before
553 being sorted as CSCs in mammosphere culture media. Interestingly, it reverted to (35.5%) at day
554 21. From these results, it is concluded that sorting of CSCs allows them to acquire stemness
555 character that is much higher than their parental cells and their unsorted population, and declines
556 over time. The interpretation is that CSCs upon repetitive and continuous growth are driven
557 towards differentiation into regular cancer cells instead of bearing a CSC state. In another
558 interpretation, a distinctive characteristic of mammosphere culture conditions -unlike the
559 adherent cell culture- is that during the passaging of CSCs most of them die early (through
560 apoptosis/anoikis) and the mitogen-responsive anoikis resistant cells that were supposed to be
561 CSCs grow and form new mammospheres. Therefore, increased expression of CD44^{+}/CD24$^{−}$

562   within mammospheres compared to parent cells could be due to an enriched anoikis-resistant

563   cancer stem cells proliferation process (Deleyrolle et al. 2011).

564   The second stage of our study was to investigate the role of cycling hypoxia on CSCs

565   propagation, stemness character, drug resistance, and adequate motility to recruit new tumor

566   growth at distant sites through migration and induction of VEGF expression level. In our study

567   as detailed in methods, we divided CSCs into two groups to be exposed to intermittent or

568   continuous shots of hypoxia. MTT cytotoxicity assay was performed to assess chemoresistance

569   of CSCs in hypoxia vs. normoxia vs. parent MCF-7 cells using doxorubicin. Doxorubicin is a

570   cytotoxic anthracycline, that is widely used drug to treat breast cancer. The cytotoxic effect of

571   doxorubicin on malignant cells is due to nucleotide base intercalation and cell membrane lipid

572   binding. Intercalation inhibits nucleotide replication and action of DNA and RNA polymerases.

573   The interaction of doxorubicin with topoisomerase II to form DNA-cleavable complexes appears

574   to be an important mechanism of doxorubicin cytocidal activity (Miglietta et al. 2000). Our

575   results have shown that parent MCF-7 had the lowest drug resistance to doxorubicin

576   (IC_{50}=0.46uM) compared to normoxic CSCs mammosphere (IC_{50}=1.90 uM), and when both

577   were compared to CSCs[HYP] that underwent hypoxic episodes of **INTR.20** and **CONT.5**, they had

578   (IC_{50}=6.20 uM) and (IC_{50}=7.12 uM), respectively. Consequently, one concludes that hypoxia

579   remarkably elevates chemoresistance not only upon comparison with parent MCF-7, but also

580   upon comparison with the CSCs[NOR] (control). It is noteworthy to explain that the IC_{50} values of

581   CSCs[HYP] subjected to all these hypoxic episodes (**INTR.10, INTR.20, INTR.30**, **CONT.5,** and

582   **CONT.10)** were higher than parental MCF-7 and than CSCs[NOR] (control), with an exception for

583   the CSCs[HYP] that underwent (**INTR.40 and CONT.15)** episodes representing the finale of the

584   hypoxic treatment which had IC_{50} values that were less than the IC_{50} of CSCs[NOR] (control) and

585   close to parental MCF-7. It is notable to compare MTT assay results with flow cytometry results

586   of the CSCs[HYP] as they reflect one another. MTT assay results for sorted CSCs have shown

587   higher chemoresistance with (4-fold) increased IC_{50} compared to parental MCF-7 whose

588   $CD44^{+}/CD24^{-}$ expression was (1%). This proposes the likelihood that increased stemness is the

589   contributor to the higher drug resistance in mammospheres as suggested previously (Calcagno et

590   al. 2010). Moreover, identification of $CD44^{+}/CD24^{-}$ expression by flow cytometry applied on

591   CSCs[HYP] that underwent **CONT.5** and **INTR.20** revealed their possession of the highest

592   expression at 51.6% and 39.8%, respectively. Among all hypoxic episodes, the lowest

593   expressions of 0.5% and 0.3% were for CSCs[HYP] that underwent **CONT.15** and **INTR.40**,

594   respectively. Interestingly, CSCs[HYP] that underwent **CONT.5** and **INTR.20,** which had the

595   highest CD44$^+$/CD24$^-$ expression also had the highest chemoresistance results in contrast to

596   **CONT.15** and **INTR.40** which had the lowest CD44$^+$/CD24$^-$ expression, and also the lowest

597   chemoresistance results. These results agree with their counterparts in past studies which showed

598   that chemoresistance is closely related to many fundamental or acquired characteristics of CSCs,

599   such as DNA repair ability, quiescence, overexpression of antiapoptotic enzymes, drug efflux

600   transporters and detoxifying enzymes (Vinogradov & Wei 2012). Our findings also agree with

601   the study of (Hermann et al. 2007) that reported the existence of a subpopulation of pancreatic

602   cancer cells which resembled stem cells and had higher gemcitabine resistance both *in vitro* and

603   *in vivo*. Since CSCs play a significant role in tumor recurrence and metastasis, wound-healing

604   was investigated to evaluate the behavior of CSCs after being exposed to different hypoxic shots.

605   The adherent CSCs^{HYP} showed greater ability of self-renewal and wound healing, especially after

606   being exposed to **INTR.20** and **CONT.5** hypoxic shots. They also showed the slowestwound

607   healing rate after being exposed to **INTR.40** and **CONT.15**. The wound healing results were

608   mirror-image reflection of the chemoresistance and stemness characteristics results relevant to

609   each hypoxic episode discussed above.

610   The third phase of this study was performed to evaluate the role of secretions of CSCs after

611   being subjected to different hypoxic shots on angiogenesis using (HUVECs) as a model

612   proposed to modulate neovascularization phenotype. Increased VEGF secretion in CSCs^{HYP}

613   versus control CSCs^{NOR} was confirmed. This finding demonstrated that CSCs^{HYP} secretions

614   increased the level of VEGF significantly which is linked to the angiogenic potential of the CdM

615   reported in this study. In this manner, the study of (Bao et al. 2006) showed that CD133$^+$

616   enriched stem cell-like glioma cells (SCLGC) produced tumors with an increased tumor

617   vascularity, necrosis, and hemorrhage. Also, the authors showed that the VEGF expression was

618   10-20 fold up-regulated in CD133$^+$ SCLGC.

619   The direct and indirect co-culture of CSCs^{HYP} that underwent **CONT.5** with endothelial

620   HUVECs proved that this co-culture system comprised constituents that promoted angiogenic

621   phenotype, such as proliferation and differentiation of endothelial cell into a net-like structure.

622   Interestingly, the influence of the secretions from CSCs^{HYP} modified the HUVECs morphology

623   to a longer, mesenchymal-like appearance and enhanced their migration rate. The migration

624   assay confirmed that CdM obtained from CSCs^{HYP} enhanced the migration rate of HUVECs

625   compared to its control group cultured in EBM-2. HUVECs migrated towards the

626   chemoattractants that CSCs^{HYP} secreted in the CdM that were obtained from all hypoxic

627   episodes, except the CdM that were obtained from **CONT.15** and **INTR.40,** which did not

628 enhance HUVECs migration. However, migration was distinctive upon the use of CdM obtained
629 from **CONT.5** and **INTR.20**. These results could be interpreted in light of the biological process
630 in which the growth of a new blood vessel from pre-existing blood cells via "sprouting" of
631 endothelial cells is led by a tip cell which is a single endothelial one. Tip cells drive vascular
632 growth by detecting gradient proangiogenic mediators such as VEGF. Adjacent endothelial cells
633 become stalk cells that can proliferate and migrate towards the tip cell which results in the
634 elongation of the sprouting vessel (Gerhardt et al. 2003).

635

636 The wound healing assay has confirmed that the CdM obtained from CSCs^{HYP} enhanced the
637 repair of the scratch in HUVECs, and closure was significantly higher upon the use of CdM
638 obtained from **CONT.5** and **INTR.20** episodes in comparison to wound closure treated with
639 CdM media obtained from CSCs^{NOR}. Moreover, the addition of CdM obtained from CSCs^{HYP}
640 cultures into HUVECs was also found to promote the endothelial cell proliferation and induce
641 capillary-like tube structure formation by increasing total length of the formed branched-tube,
642 the number of loops and the area covered by the tubes. This observation was distinctive in the
643 use of CdM obtained from CSCs^{HYP} exposed to **CONT.5** and to **INTR.20**. Together, these
644 results suggest that CSCs^{HYP} cells produce pro-angiogenic factors that may directly alter the
645 behavior of endothelial cells. Such findings are in agreement with the study of (Tu et al. 2009)
646 which showed that A549 lung cancer cells hypoxic CdM improved HUVECs' cell presence and
647 wound healing migration ability.

648

649 In conclusion, the angiogenic components and the angiogenic switch were enhanced by the
650 tumor microenvironment constructed by the CdM of CSCs^{HYP} particularly after 5 hypoxic
651 episodes of continuous 72-hours weekly exposure (**CONT.5**) and 20 episodes of intermittent 8-
652 hours exposure to hypoxia, 3 times weekly (**INTR.20**).

653

654 In the context of the above-detailed findings and upon comparing the results of CSCs exposed to
655 intermittent versus continuous hypoxic condition in terms of stemness, chemoresistance, tube
656 formation and VEGF protein expression related to angiogenesis, wound healing and finally, cell
657 migration, the results implied similarity among intermittent and continuous treatments between
658 the early intervals **(INTR.20 and CONT.5)**, between the intermediate intervals **(INTR.30 and
659 CONT.10)**, and also between the late intervals **(INTR.40 and CONT.15).**
660 The present study agrees with the study of   (Liu et al. 2017) which demonstrated that
661 intermittent and continuous hypoxic conditions significantly increased the migration of
662 MDA-MB-231 breast cancer cells to a certain extent, either because of excessive long-term

663   exposure or because of the increased number of hypoxia-reoxygenation cycles. In this study, the
664   maximum increase of these features by hypoxic effect was observed at early intervals **(INTR.20**
665   **and CONT.5),** whereas it started to decline at intermediate ones **(INTR.30 and CONT.10)**, and
666   drastically declined at late intervals **(INTR.40 and CONT.15)** to a rate even lower than the
667   control group of CSCs in normoxia

668   The previous study demonstrated that excessive long-term or high-frequency exposure to
669   hypoxia leads to the generation of reactive oxygen species (ROS), which in turn, induces lipid
670   peroxidation and increases the production of stress responding proteins, thus promotes DNA
671   strand breakage, cellular injury, and apoptosis (Pires et al. 2010; Zepeda et al. 2013). Generally,
672   low levels of ROS are required for stem cells to maintain quiescence and self-renewal.
673   Therefore, in the CSCs scenario, a low concentration of ROS enhances their stemness and
674   contributes to tumorigenesis (Liu & Wang 2015). However, increased ROS production due to
675   extensive hypoxia causes CSCs exhaustion, differentiation, senescence, and apoptosis (Zhou et
676   al. 2014).

677   Thus, it is interpreted that the ROS level began to increase starting from the intermediate
678   intervals **(INTR.30 and CONT.10)** and reached maximal rate in the late intervals **(INTR.40 and**
679   **CONT.15)** proposing the manifestation of differentiation, senescence, and apoptosis in CSCs
680   extensively exposed to hypoxia, based on the previous explanation.

681
682

683   **CONCLUSION**

684

685   This study has proven that the highly optimized hypoxia-reoxygenation system applied to CSCs
686   has enriched their growth, enhanced their properties of self-renewal, increased the expression of
687   stemness surface markers, and increased their chemoresistance. The findings of this study also
688   demonstrated that the CSCs[HYP] microenvironment plays a major role in enhancing angiogenesis
689   and tumor vascularization by recruiting endothelial cells into the tumor microenvironment, and
690   in activating distinct molecular mechanisms that need further investigations. Whether the
691   elevation of stemness in CSCs[HYP] results from the de-differentiation of differentiated MCF-7
692   cells, or from the enhanced proliferation of CSCs after hypoxic exposure is still unclear and
693   needs further studies. The interactions between CSCs in tumor microenvironment and other
694   contributing processes such as hypoxia and angiogenesis are still at the infancy stage and need
695   in-depth future research.

696

697 **REFERENCES**

698 Al-Hajj M, Wicha MS, Benito-Hernandez A, Morrison SJ, and Clarke MF. 2003. Prospective
699   identification of tumorigenic breast cancer cells. *Proceedings of the National Academy of*
700   *Sciences* 100:3983-3988.
701 Bao S, Wu Q, Sathornsumetee S, Hao Y, Li Z, Hjelmeland AB, Shi Q, McLendon RE, Bigner
702   DD, and Rich JN. 2006. Stem cell–like glioma cells promote tumor angiogenesis through
703   vascular endothelial growth factor. *Cancer research* 66:7843-7848.
704 Batlle E, and Clevers H. 2017. Cancer stem cells revisited. *Nature medicine* 23:1124.
705 Bristow RG, and Hill RP. 2008. Hypoxia and metabolism: hypoxia, DNA repair and genetic
706   instability. *Nature Reviews Cancer* 8:180.
707 Brurberg KG, Graff BA, Olsen DR, and Rofstad EK. 2004. Tumor-line specific pO2 fluctuations
708   in human melanoma xenografts. *International Journal of Radiation Oncology• Biology•*
709   *Physics* 58:403-409.
710 Calcagno AM, Salcido CD, Gillet J-P, Wu C-P, Fostel JM, Mumau MD, Gottesman MM,
711   Varticovski L, and Ambudkar SV. 2010. Prolonged drug selection of breast cancer cells
712   and enrichment of cancer stem cell characteristics. *Journal of the National Cancer*
713   *Institute* 102:1637-1652.
714 Cassavaugh J, and Lounsbury KM. 2011. Hypoxia-mediated biological control. *Journal of*
715   *cellular biochemistry* 112:735-744.
716 Chaplin DJ, Olive PL, and Durand RE. 1987. Intermittent blood flow in a murine tumor:
717   radiobiological effects. *Cancer research* 47:597-601.
718 Chenevier-Gobeaux C, Simonneau C, Lemarechal H, Bonnefont-Rousselot D, Poiraudeau S,
719   Rannou F, Ekindjian O, Anract P, and Borderie D. 2013. Effect of hypoxia/reoxygenation
720   on the cytokine-induced production of nitric oxide and superoxide anion in cultured
721   osteoarthritic synoviocytes. *Osteoarthritis and cartilage* 21:874-881.
722 Crowder SW, Balikov DA, Hwang Y-S, and Sung H-J. 2014. Cancer stem cells under hypoxia as
723   a chemoresistance factor in the breast and brain. *Current pathobiology reports* 2:33-40.
724 Deleyrolle LP, Ericksson G, Morrison BJ, Lopez JA, Burrage K, Burrage P, Vescovi A, Rietze
725   RL, and Reynolds BA. 2011. Determination of somatic and cancer stem cell self-
726   renewing symmetric division rate using sphere assays. *PloS one* 6:e15844.
727 Denko NC. 2008. Hypoxia, HIF1 and glucose metabolism in the solid tumour. *Nature Reviews*
728   *Cancer* 8:705.
729 Eales K, Hollinshead K, and Tennant D. 2016. Hypoxia and metabolic adaptation of cancer cells.
730   *Oncogenesis* 5:e190.
731 Gerhardt H, Golding M, Fruttiger M, Ruhrberg C, Lundkvist A, Abramsson A, Jeltsch M,
732   Mitchell C, Alitalo K, and Shima D. 2003. VEGF guides angiogenic sprouting utilizing
733   endothelial tip cell filopodia. *The Journal of cell biology* 161:1163-1177.
734 Gordan JD, Lal P, Dondeti VR, Letrero R, Parekh KN, Oquendo CE, Greenberg RA, Flaherty
735   KT, Rathmell WK, and Keith B. 2008. HIF-α effects on c-Myc distinguish two subtypes

736   of sporadic VHL-deficient clear cell renal carcinoma. *Cancer cell* 14:435-446.

737   Hammer S, To KK, Yoo Y-G, Koshiji M, and Huang LE. 2007. Hypoxic suppression of the cell
738   cycle gene CDC25A in tumor cells. *Cell Cycle* 6:1919-1926.

739   Hermann PC, Huber SL, Herrler T, Aicher A, Ellwart JW, Guba M, Bruns CJ, and Heeschen C.
740   2007. Distinct populations of cancer stem cells determine tumor growth and metastatic
741   activity in human pancreatic cancer. *Cell stem cell* 1:313-323.

742   Huang R, and Rofstad EK. 2017. Cancer stem cells (CSCs), cervical CSCs and targeted
743   therapies. *Oncotarget* 8:35351.

744   Kaur B, Khwaja FW, Severson EA, Matheny SL, Brat DJ, and Van Meir EG. 2005. Hypoxia and
745   the hypoxia-inducible-factor pathway in glioma growth and angiogenesis. *Neuro-
746   oncology* 7:134-153.

747   Kerbel RS. 2008. Tumor angiogenesis. *New England Journal of Medicine* 358:2039-2049.

748   Kietzmann T, Mennerich D, and Dimova EY. 2016. Hypoxia-inducible factors (HIFs) and
749   phosphorylation: impact on stability, localization, and transactivity. *Frontiers in cell and
750   developmental biology* 4:11.

751   Kong W, He L, Richards E, Challa S, Xu C, Permuth-Wey J, Lancaster J, Coppola D, Sellers T,
752   and Djeu J. 2014. Upregulation of miRNA-155 promotes tumour angiogenesis by
753   targeting VHL and is associated with poor prognosis and triple-negative breast cancer.
754   *Oncogene* 33:679.

755   Kruyt FA, and Schuringa JJ. 2010. Apoptosis and cancer stem cells: Implications for apoptosis
756   targeted therapy. *Biochemical pharmacology* 80:423-430.

757   Lin S-P, Lee Y-T, Wang J-Y, Miller SA, Chiou S-H, Hung M-C, and Hung S-C. 2012. Survival
758   of cancer stem cells under hypoxia and serum depletion via decrease in PP2A activity and
759   activation of p38-MAPKAPK2-Hsp27. *PLoS one* 7:e49605.

760   Liu J, and Wang Z. 2015. Increased oxidative stress as a selective anticancer therapy. *Oxidative
761   medicine and cellular longevity* 2015.

762   Liu L, Liu W, Wang L, Zhu T, Zhong J, and Xie N. 2017. Hypoxia‑inducible factor 1 mediates

763   intermittent hypoxia‑induced migration of human breast cancer MDA‑MB‑231 cells.

764   *Oncology letters* 14:7715-7722.

765   Mellor H, Snelling S, Hall M, Modok S, Jaffar M, Hambley T, and Callaghan R. 2005. The
766   influence of tumour microenvironmental factors on the efficacy of cisplatin and novel
767   platinum (IV) complexes. *Biochemical pharmacology* 70:1137-1146.

768   Miglietta A, Cavalli R, Bocca C, Gabriel L, and Gasco MR. 2000. Cellular uptake and
769   cytotoxicity of solid lipid nanospheres (SLN) incorporating doxorubicin or paclitaxel.
770   *International journal of pharmaceutics* 210:61-67.

771   Muz B, de la Puente P, Azab F, and Azab AK. 2015. The role of hypoxia in cancer progression,
772   angiogenesis, metastasis, and resistance to therapy. *Hypoxia* 3:83.

773   Ojha T, Pathak V, Shi Y, Hennink WE, Moonen CT, Storm G, Kiessling F, and Lammers T.
774   2017. Pharmacological and physical vessel modulation strategies to improve EPR-
775   mediated drug targeting to tumors. *Advanced drug delivery reviews* 119:44-60.

776   Peitzsch C, Tyutyunnykova A, Pantel K, and Dubrovska A. 2017. Cancer stem cells: the root of
777   tumor recurrence and metastases. Semin Cancer Biol: Elsevier. p 10-24.

778   Ping YF, and Bian XW. 2011. Concise review: contribution of cancer stem cells to
779   neovascularization. *Stem Cells* 29:888-894.

780   Pires IM, Bencokova Z, Milani M, Folkes LK, Li J-L, Stratford MR, Harris AL, and Hammond
781   EM. 2010. Effects of acute versus chronic hypoxia on DNA damage responses and
782   genomic instability. *Cancer research*:0008-5472. CAN-0009-2715.

783   Senthebane DA, Rowe A, Thomford NE, Shipanga H, Munro D, Al Mazeedi MA, Almazyadi
784   HA, Kallmeyer K, Dandara C, and Pepper MS. 2017. The role of tumor
785   microenvironment in chemoresistance: To survive, keep your enemies closer.
786   *International journal of molecular sciences* 18:1586.

787   Tu ML, Wang HQ, Chen LJ, Lu JC, Jiang F, Liang JH, and Li DS. 2009. Involvement of
788   Akt1/protein kinase Bα in tumor conditioned medium-induced endothelial cell migration
789   and survival in vitro. *Journal of cancer research and clinical oncology* 135:1543-1550.

790   Vinogradov S, and Wei X. 2012. Cancer stem cells and drug resistance: the potential of
791   nanomedicine. *Nanomedicine* 7:597-615.

792   Wang L, Zhang L, Shen W, Liu Y, and Luo Y. 2016. High expression of VEGF and PI3K in
793   glioma stem cells provides new criteria for the grading of gliomas. *Experimental and*
794   *therapeutic medicine* 11:571-576.

795   Wang Z, Butner JD, Kerketta R, Cristini V, and Deisboeck TS. 2015. Simulating cancer growth
796   with multiscale agent-based modeling. Seminars in cancer biology: Elsevier. p 70-78.

797   Zepeda AB, Pessoa Jr A, Castillo RL, Figueroa CA, Pulgar VM, and Farías JG. 2013. Cellular
798   and molecular mechanisms in the hypoxic tissue: role of HIF-1 and ROS. *Cell*
799   *biochemistry and function* 31:451-459.

800   Zhao Y, and Adjei AA. 2015. Targeting angiogenesis in cancer therapy: moving beyond vascular
801   endothelial growth factor. *The oncologist* 20:660-673.

802   Zhou D, Shao L, and Spitz DR. 2014. Reactive oxygen species in normal and tumor stem cells.
803   *Advances in cancer research*: Elsevier, 1-67.

804

Figure 1

Summary of methodology workflow adopted in this project

The first stage was to establish CSCs sub-population from parental MCF-7 cells by several steps of culturing cells in ultra-low serum-free media and sorting to enrich stemness biomarker that was finally identified by flow cytometry after 21 days. Stage two included exposing CSCs to hypoxic and normoxic conditions in optimized intervals for over than four months and collecting conditioned starvation media in which they were grown. Also, multiple assays were performed using hypoxic and normoxic CSCs to test the hypoxia effect on CSCs. Stage three was performed to assess the effect of CSCs secretions in the conditioned-medium on angiogenesis.
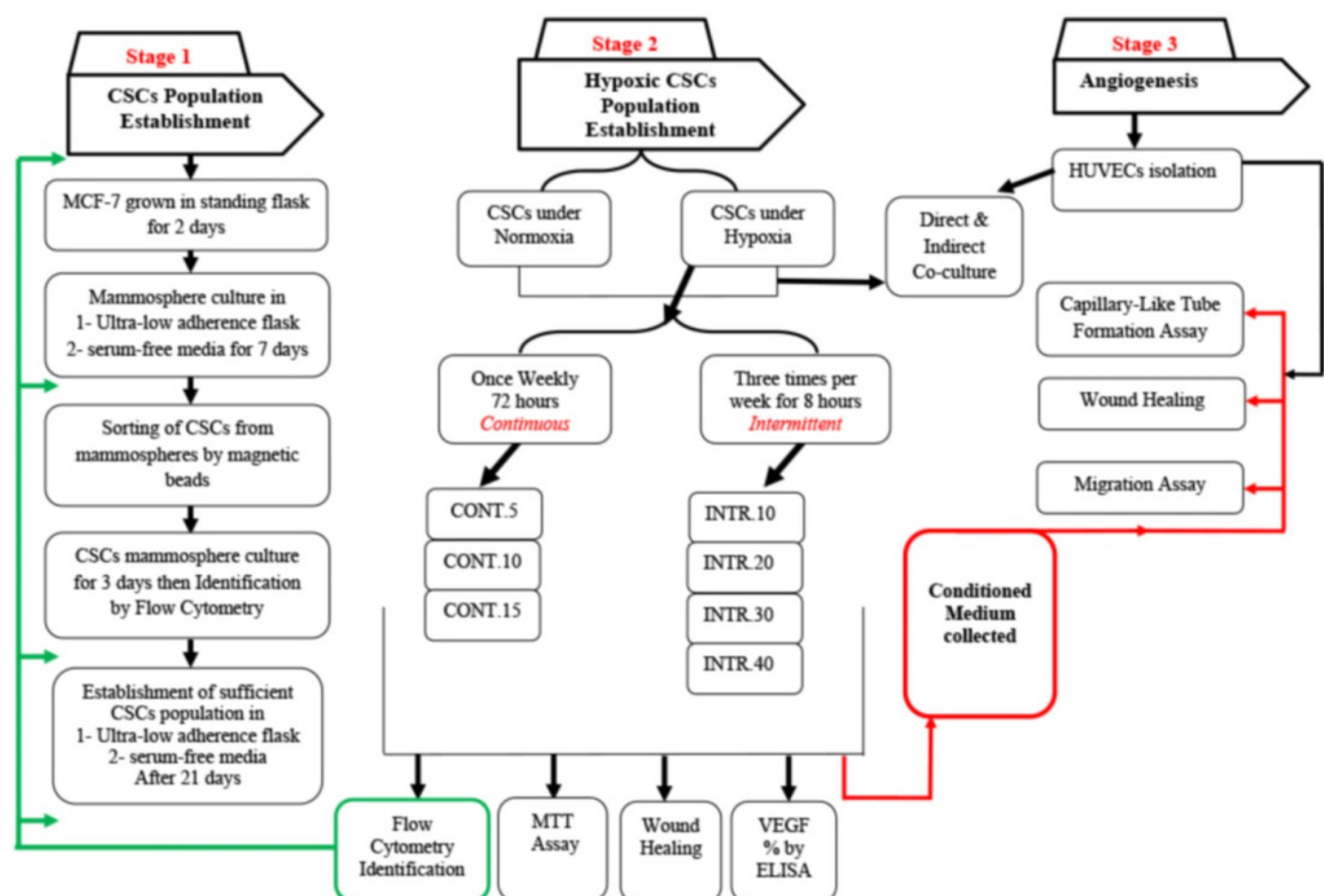
Figure 2

The morphology of MCF-7 mammospheres

(A) MCF-7 floating cells in serum-free low adherent conditions required for mammospheres formation. **(B)** At Day-3 the *(3D)* mammospheres began to structure. **(C)** At Day-7 larger and denser *(3D)* mammospheres have structured in a rigid and compact form. *Representative images* magnification (10x objective) and 30 um *scale bar by Olympus inverted microscope.*
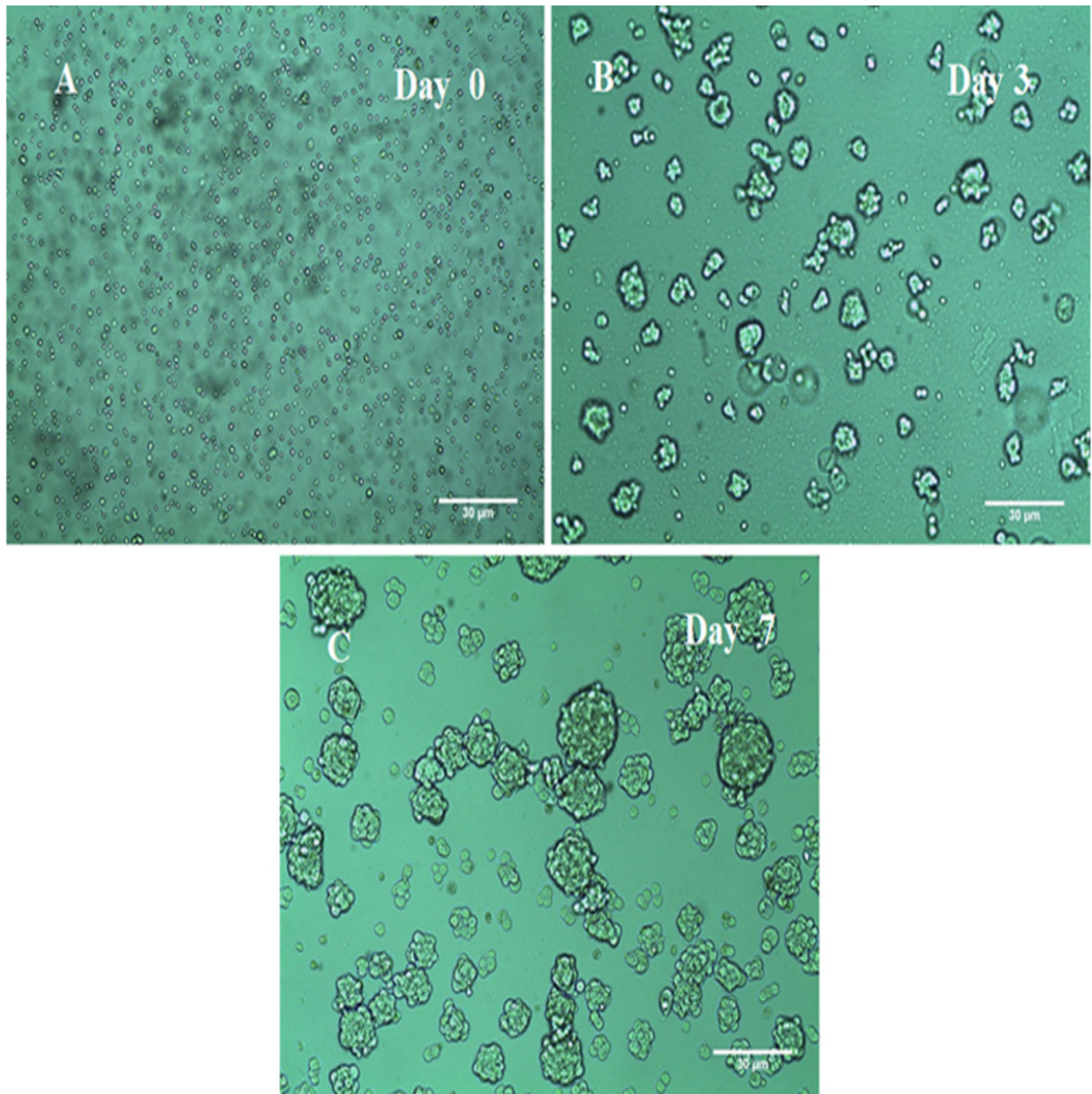
Figure 3

The 3D morphology of CSCs mammospheres under hypoxic condition (B, C, D, E) or in normoxia as in (A).

The (3D) morphology of CSCs clustered in multicellular spheroids in serum-free media. **(A)** CSCs under normoxia. **(B)** and **(C)** CSCs exposed to INTR.20 and INTR.40 hypoxic shots respectively. **(D)** and **(E)** CSCs exposed to **CONT.5** and **CONT.15** hypoxic shots respectively. CSCs^{HYP} that underwent **CONT.5** and **INTR.20** were denser and larger in number than CSCs^{NOR}. CSCs^{HYP} that underwent **CONT.15** and **INTR.40** had the least growth compared to other hypoxic exposures and CSCs^{NOR} . Representative images magnification (10x objective) and 30 um scale bar by Olympus inverted microscope.
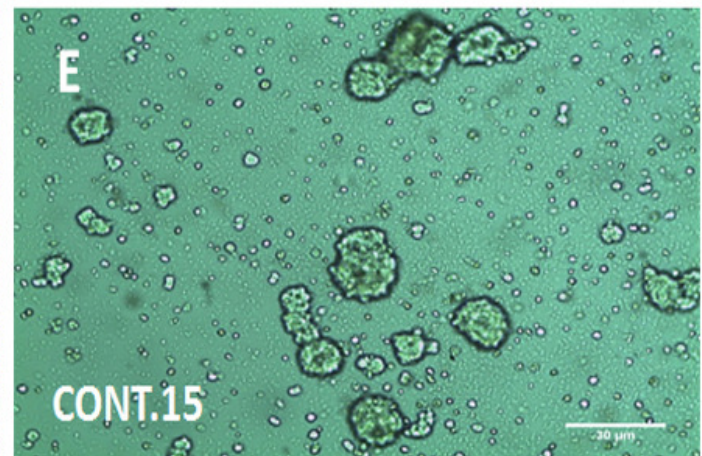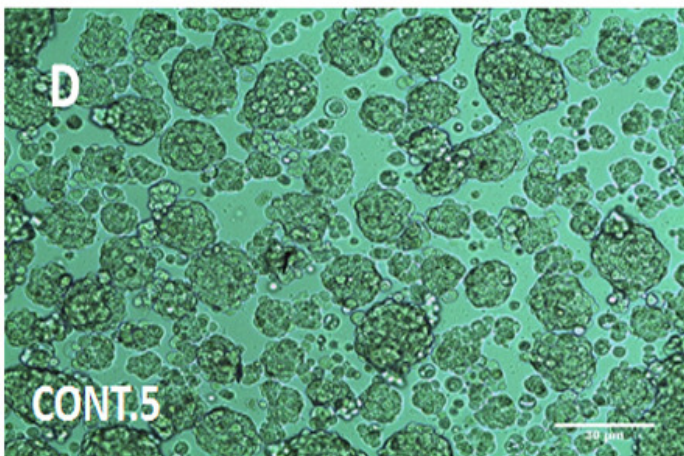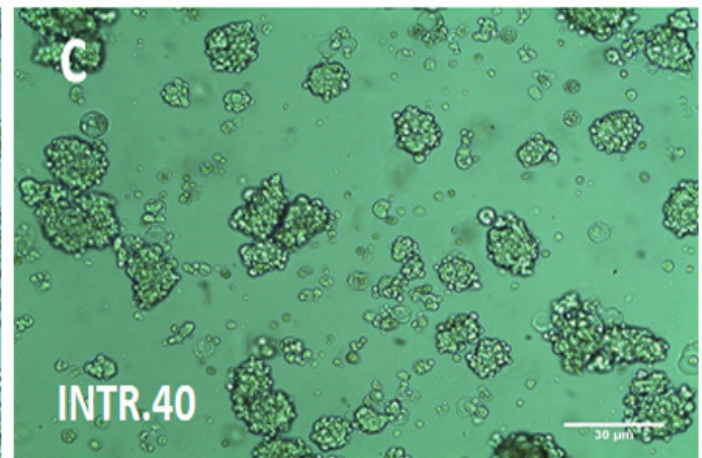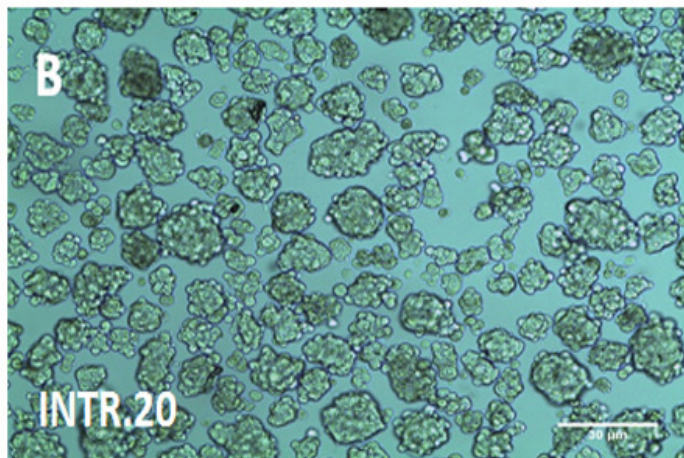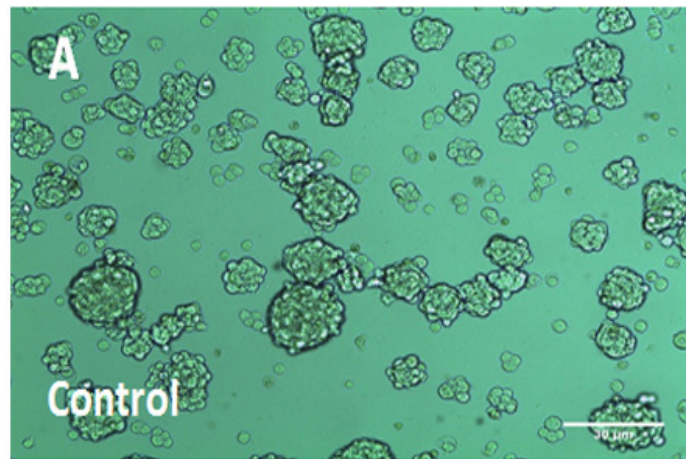
Figure 4

Determination of the cancer stem cell-like properties in mammosphere forming cells based on surface marker CD44$^+$/CD24$^-$

(A) parent MCF-7 cells. **(B)** unsorted mammospheres. **(C)** sorted CSCs mammospheres after 3 days of sorting. **(D)** CSCs mammospheres after 21 days of sorting. **(E)** CSCs^{HYP} underwent **INTR.20** shots. **(F)** CSCs^{HYP} underwent **CONT.5** shots. **(G)** CSCs^{HYP} underwent **INTR.40** shots. **(H)** CSCs^{HYP} underwent CONT.15 shots.
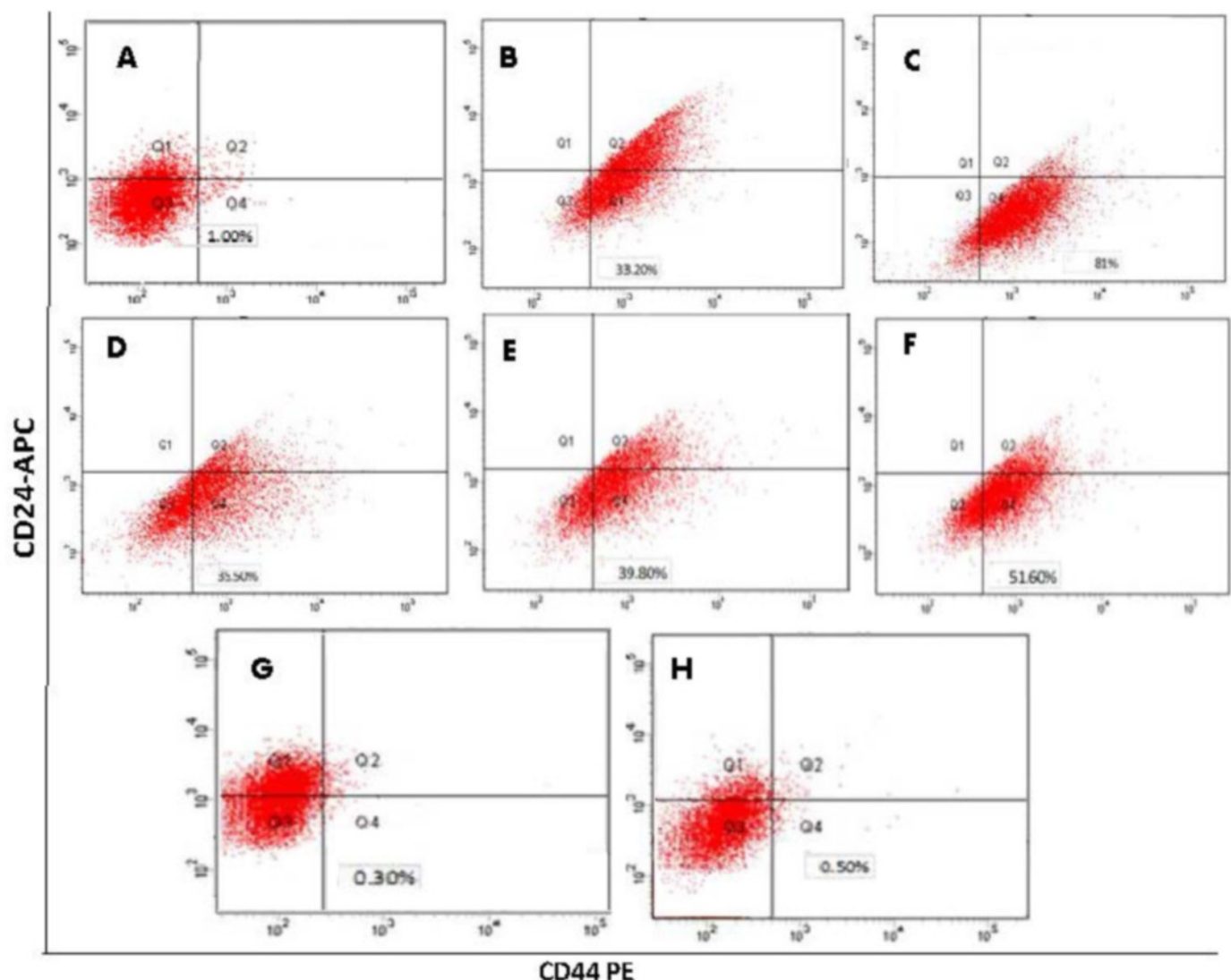
Figure 5

Effect of normoxic and hypoxic CdM on capillary-like tube structure formation in HUVECs.

HUVECs were cultured in CdM obtained from CSCs[HYP] mammospheres that were previously grown and exposed to **(B)** CONT.5 **(C)** CONT.10 **(D)** CONT.15 **(E)** INTR.10 **(F)** INTR.20 **(G)** INTR.30 **(H)** INTR.40 hypoxic shots and compared to HUVECs cultured using CdM obtained from CSCs[NOR] as a control as shown in **(A)**. Capillary-like tubular structures were the highest in using CdM obtained from **CONT.5** and **INTR.20** exposure. *Representative images magnification (4x objective) Olympus inverted microscope*
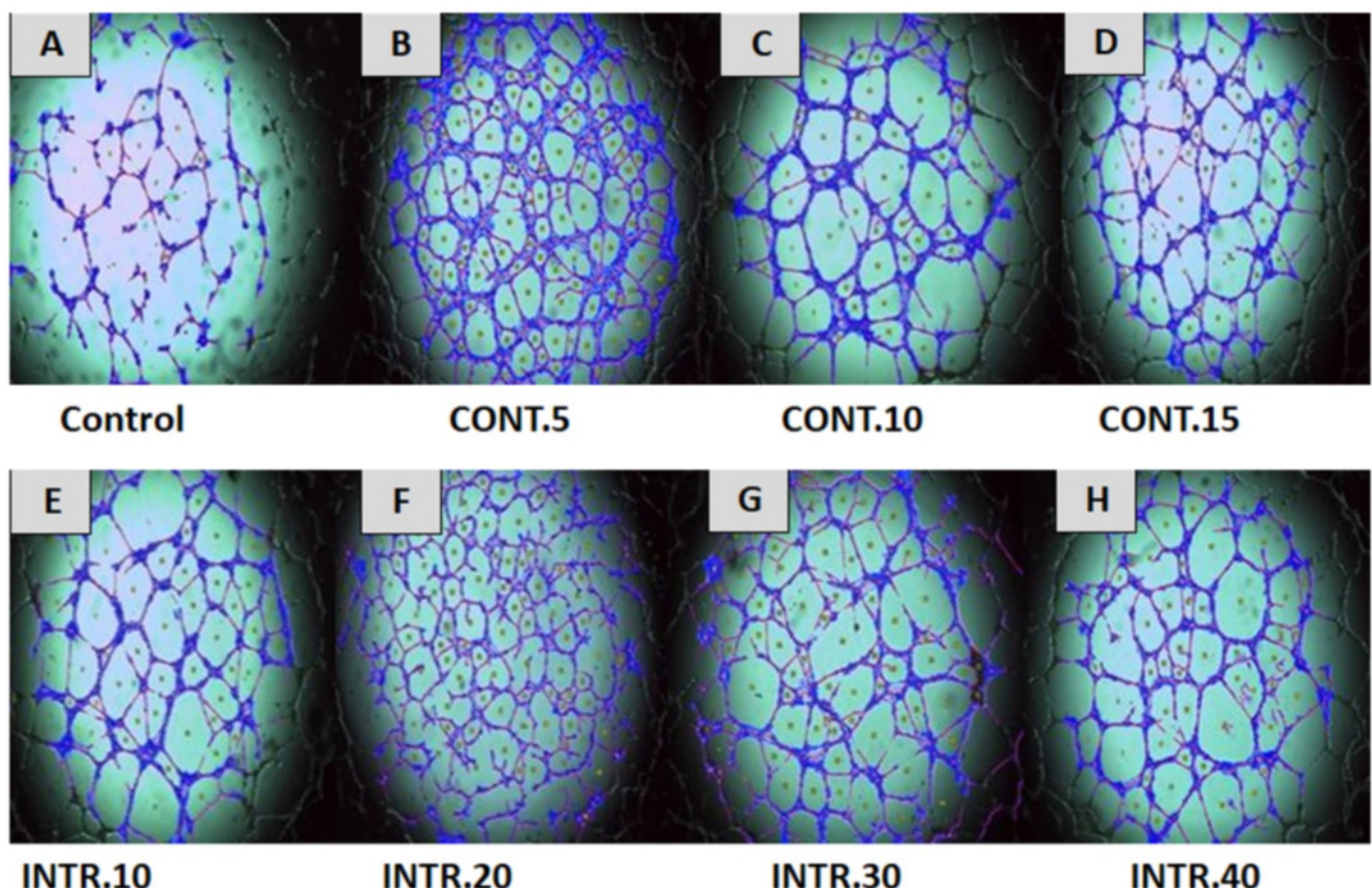
Figure 6

Assessment of capillary-like tubular structure formation

(A) Total tube lengths formed. **(B)** Number of loops intersections. **(C)** Covered area percentage. The results represent mean ± SD of three independent experiments. The symbol marks the statistical significance levels as follows: (*) indicates p<(0.001) and(**) indicates p<(0.0001) as compared to the control.
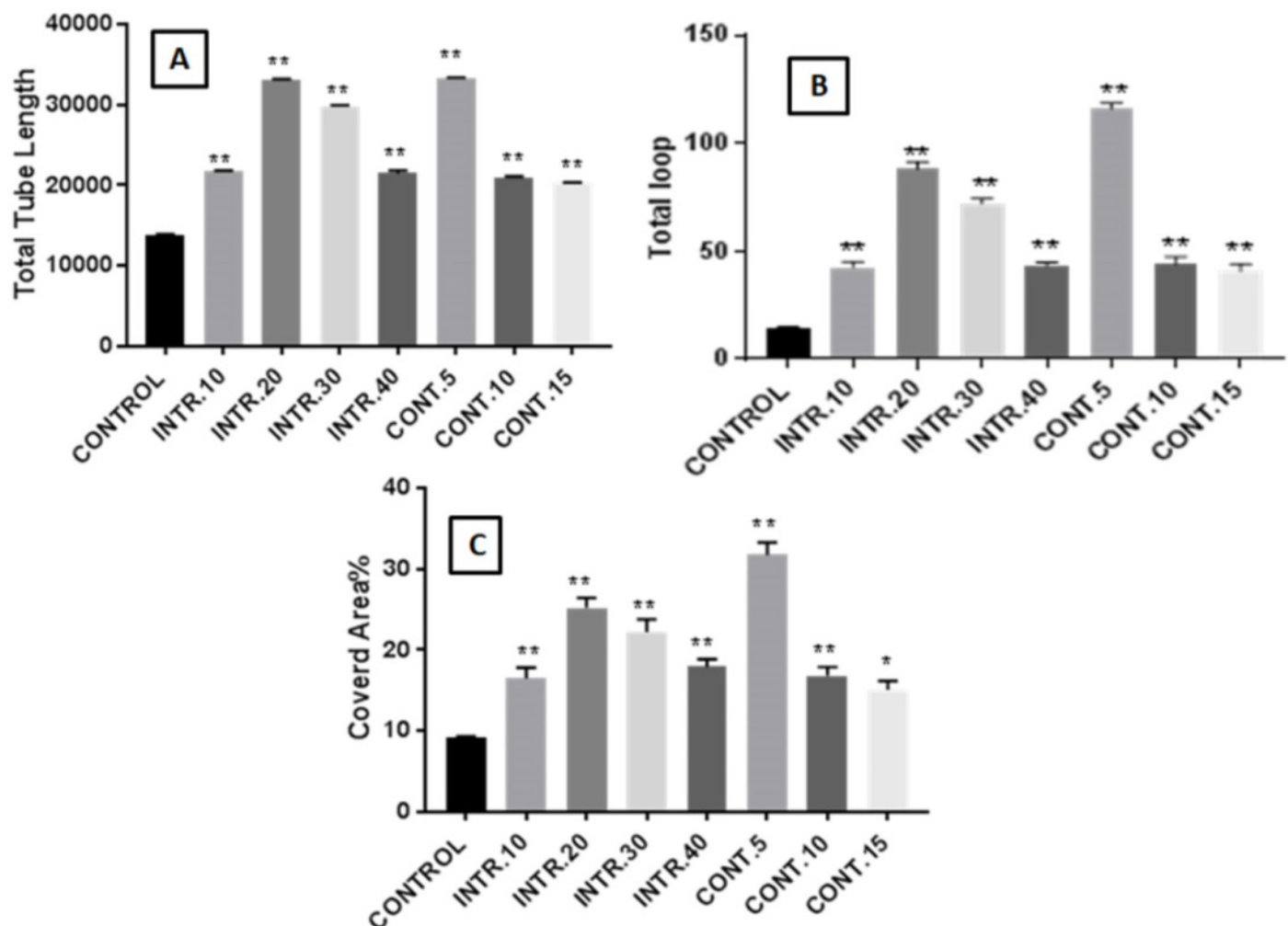
Figure 7

VEGF-A concentrations secreted by CSCs^{HYP} or CSCs^{NOR} were determined by ELISA assay

The results represent mean±SD of three independent experiments. Statistically significant differences among the treated versus control cells are shown by (*) (p ˂ 0.05) and (**) (p ˂ 0.0001).
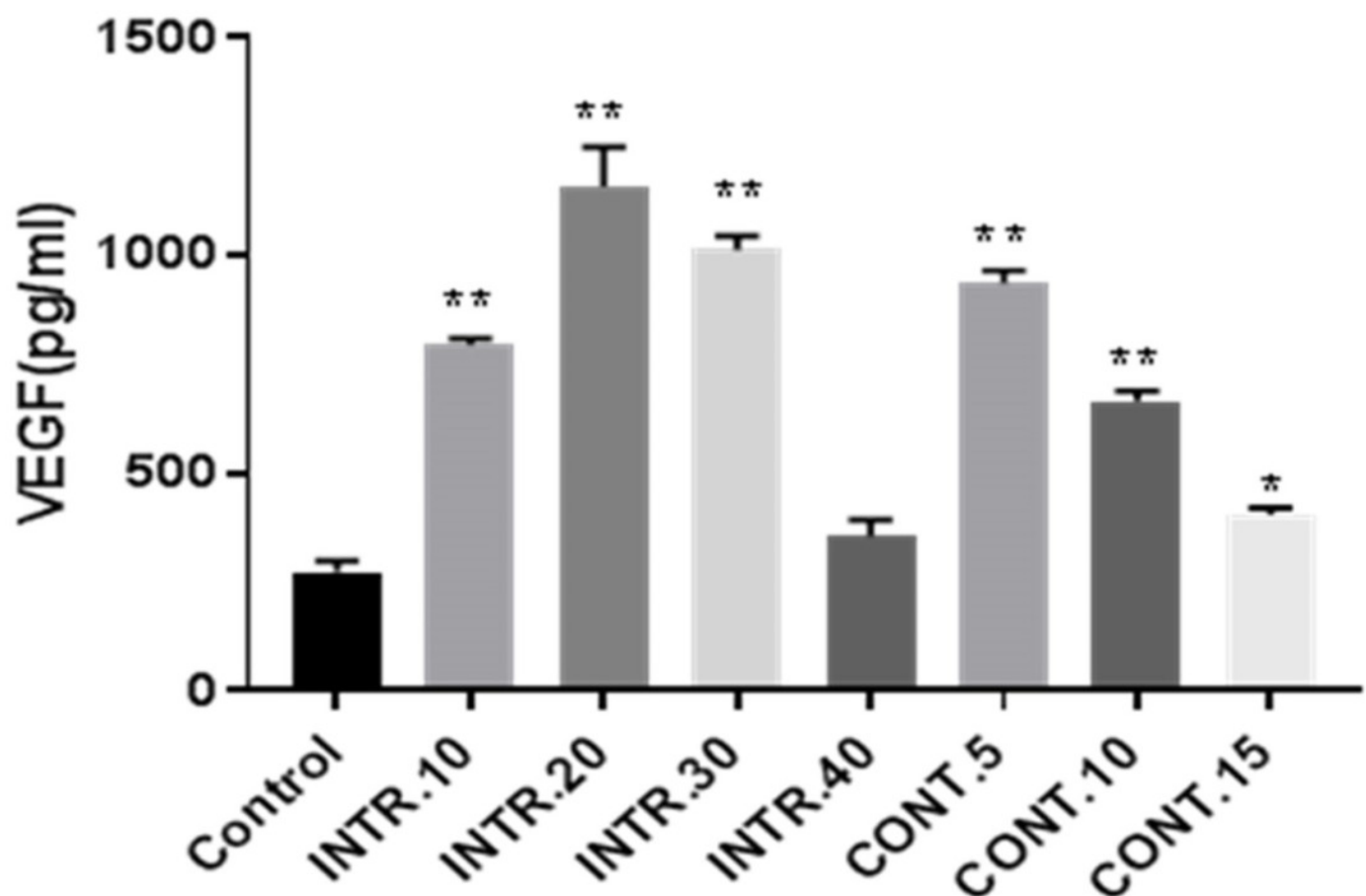
Figure 8

Transmigration of HUVECs induction by CdM obtained from CSCs[HYP] compared to control where EBM-2 serum-free served as control.

CdM from hypoxic shots **CONT.5** and **INTR.20** proved to be a potent chemoattractant compared to the control. All values were determined as averages of three independent experiments. The results represent mean±SD of three independent experiments. Statistically significant differences among the treated and control cells are shown by (**) ($p < 0.0001$).
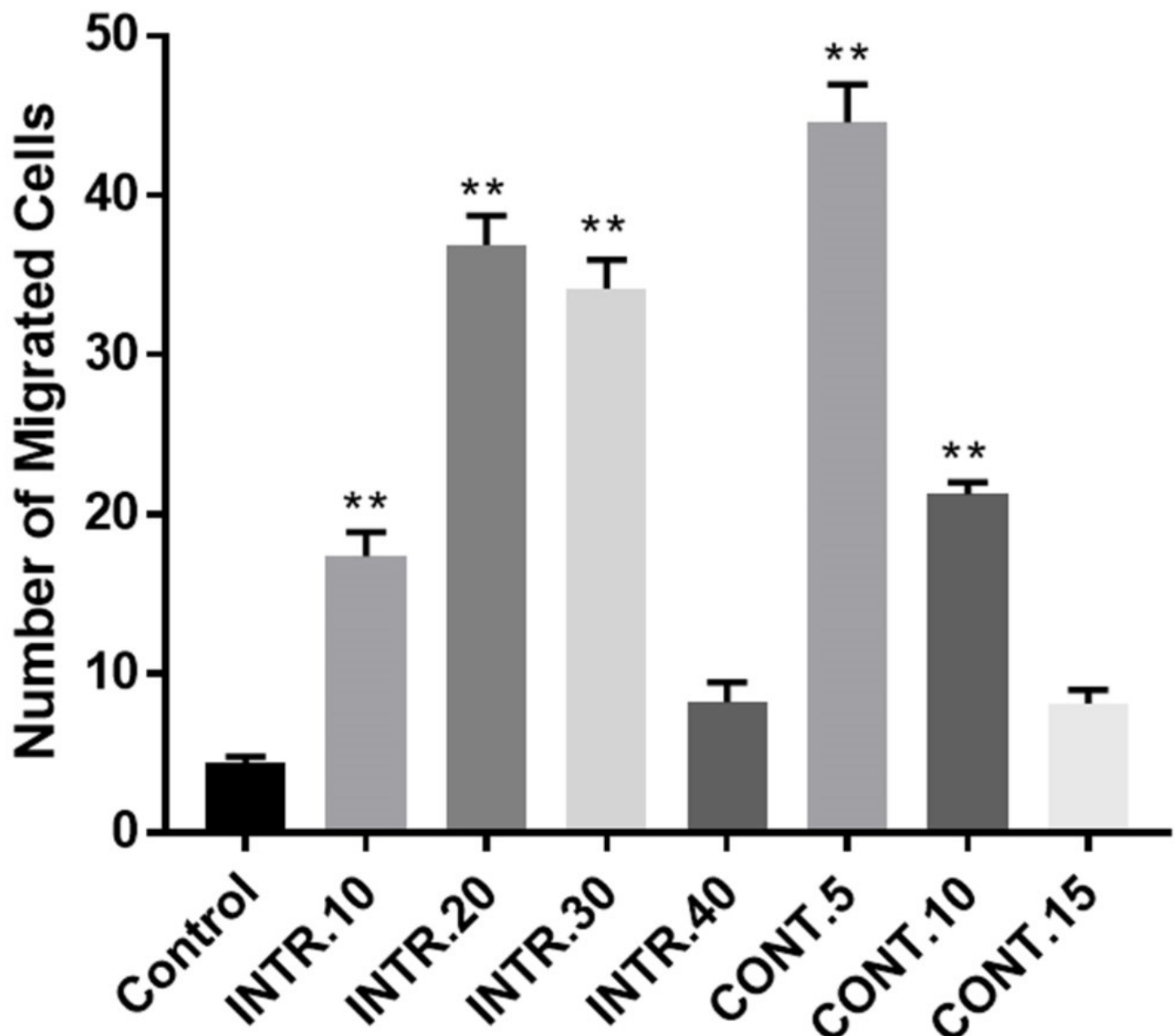
Figure 9

Morphological changes of HUVECs after co-cultured with CSCs^{HYP} subpopulation that underwent CONT.5

Hypoxic episode (**A-C**) for direct co-culture and (D-E) for indirect co-culture. Direct co-culture model: **(A)** CSCs^{HYP} mammospheres were seeded directly above HUVECs monolayer at (0) time. **(B)** After 36 hours HUVECs proliferate normally with CSCs^{HYP} . **(C)** at 72 hours HUVECs obtained elongated threadlike shape mediated by CSCs^{HYP} secretions. Indirect co-culture where permeable membrane was placed between HUVECs and **CONT.5** CSCs^{HYP} subpopulation: **(D)** HUVECs after 36 hours. **(E)** At 72 hours HUVECs morphology changed to form net-like structures resembling a vascular network as mediated by CSCs^{HYP} secretions that passed through the membrane. Representative images magnification (4x objective) Olympus inverted microscope.
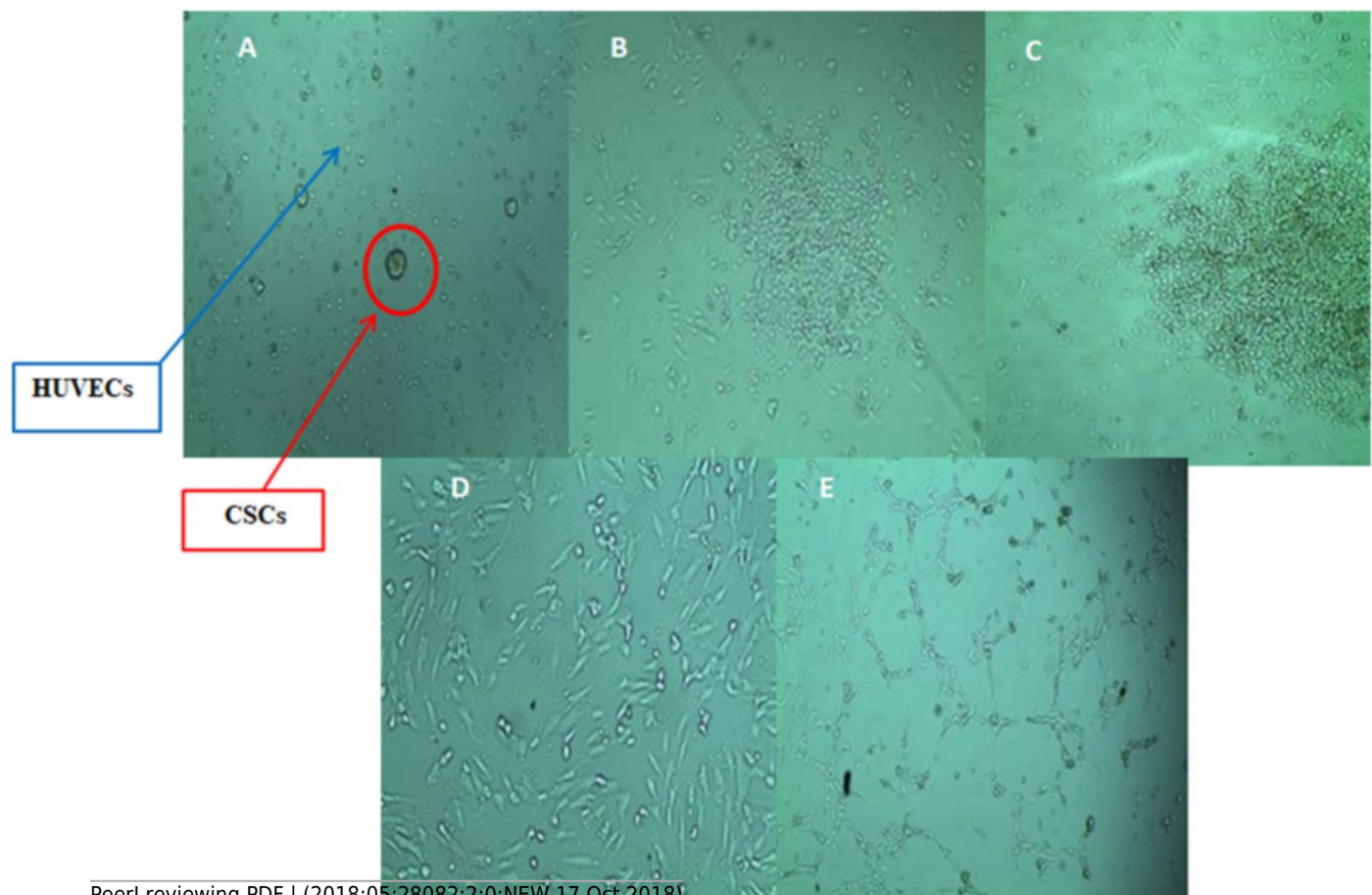
Figure 10

HUVECs cell migration assessment using wound-healing assay

The upper group of images represents the wound at zero time of treatment with CdM while lower images represent the wound after 48 hours of treatment with CdM. **(A)** control treated with CdM obtained from CSCs[NOR] . **(B)** Treated with CdM from **INTR.20** shot. **(C)** Treated with CdM from **CONT.5** shot. Representative images magnification (4x objective) Olympus inverted microscope.

0 Hour

48 Hour

Control   INTR.20   CONT.5
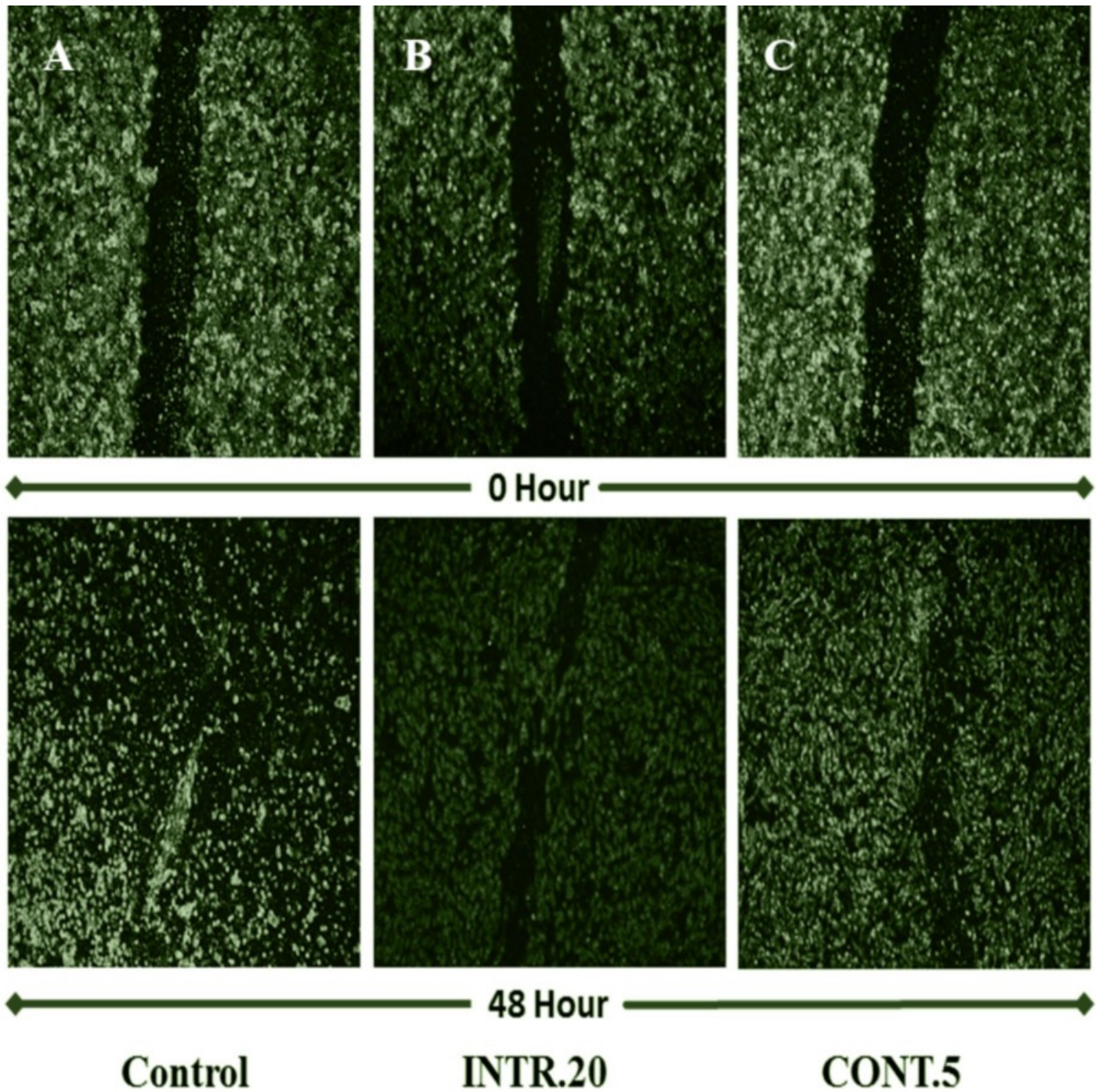
Figure 11

Wound healing of CSCs

The upper group of images demonstrate the wound surface area of CSCs monolayer at the time of wound scratching (zero time). The lower group of images are for wound closure after 36 hours from scratching. **(A)** CSCs^{NOR} used as control. **(B-H)** CSCs^{HYP} exposed to various hypoxic treatments. CSCs^{HYP} that were exposed to **INTR.20** shown in **(C)** and **CONT.5** shown in **(F)** both have had the highest wound closure capacity compared to the control CSCs^{NOR} in **(A).** *Representative images magnification (4x objective) Olympus inverted microscope.*
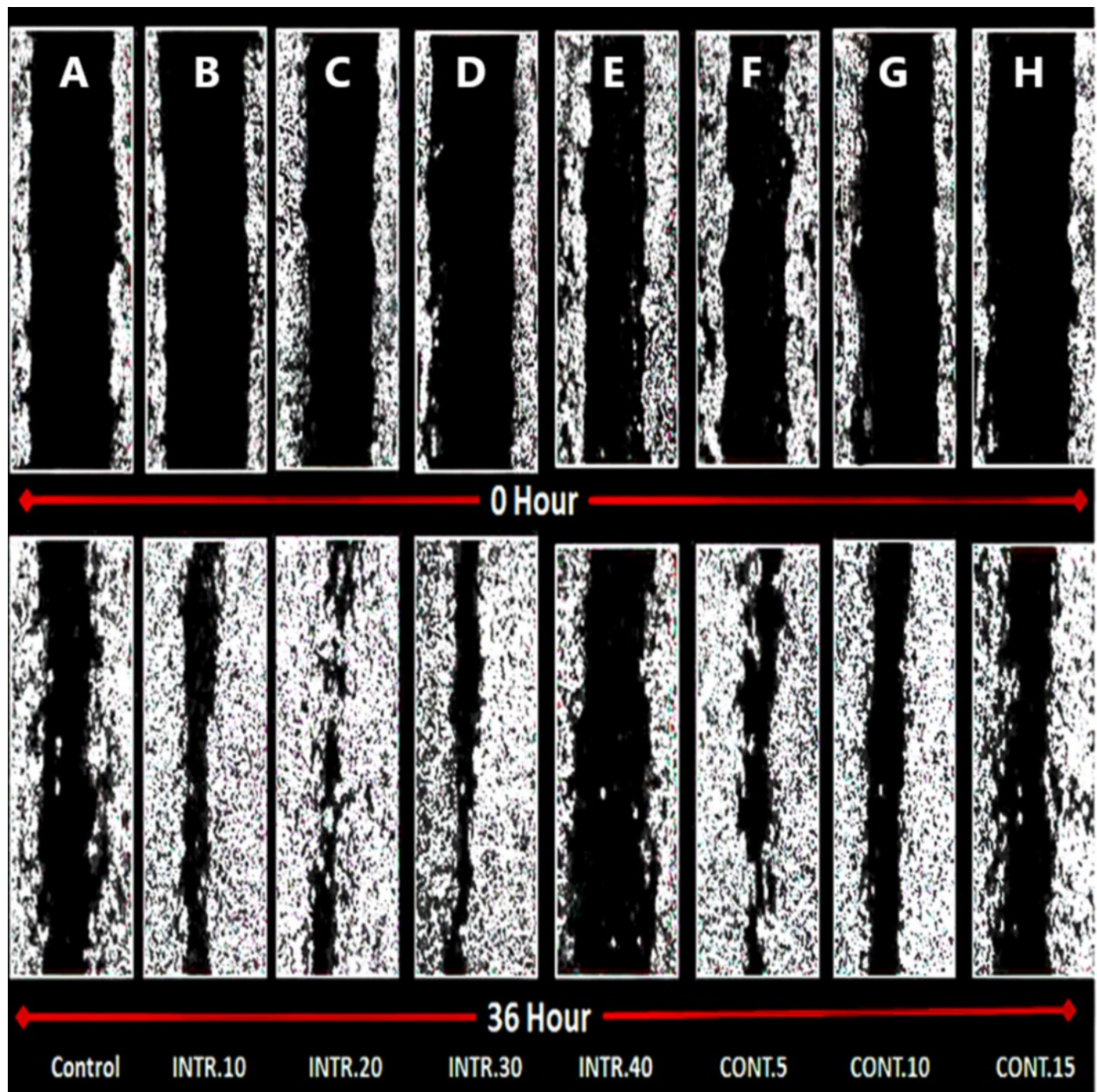
Figure 12

CSCs wound closure quantification

The quantification of wound closure was measured by ImageJ software and represented in bars expressing the percentage of gap closure. CSCs^{HYP} subpopulation that was exposed to **INTR.20** or **CONT.5** manifested the highest wound closure capacity compared to the control CSCs^{NOR}. After 36 hours, the wound closure was 98% for **INTR.20** and 95% for **CONT.5** whereas 40% for control. The results represent mean±SD of three independent experiments. Statistically significant differences among the treated and control cells are shown by (*) (p ‹ 0.001) and (**) (p ‹ 0.0001).
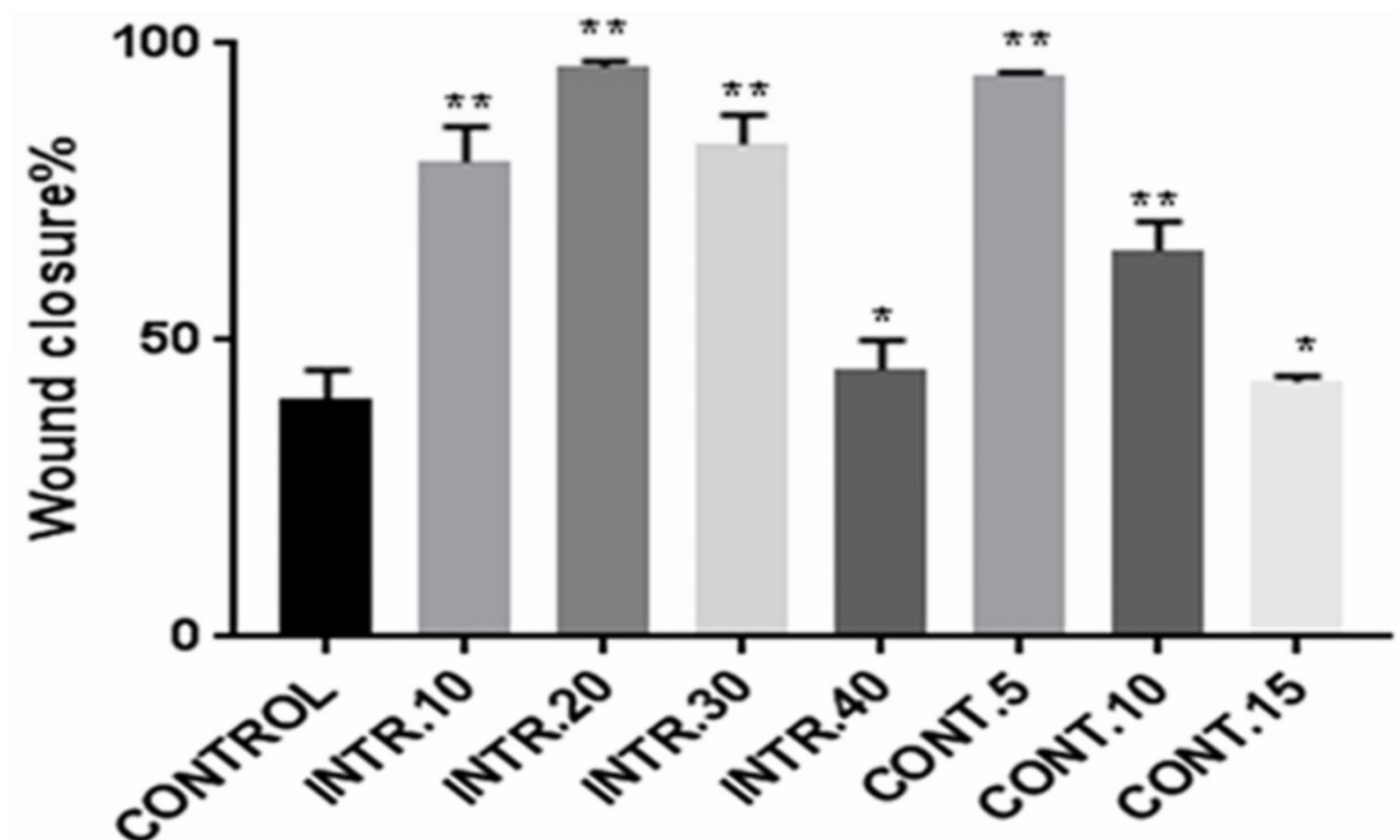
The summary of CD44$^+$/CD24$^-$ expression obtained by flow cytometry among different MCF-7 sub-population derived cells.

Cells Subpopulation	CD44$^+$/CD24$^-$ Expression %
Parent MCF-7 Cells	1.0 (± 0.1%)
Unsorted Mammospheres (Day 7 in ultra-low attachment, serum free media)	33.2 (± 3.0%)
Sorted CSCs mammospheres (3 days after sorting)	81.0 (± 7.5%)
Sorted CSCs mammospheres (After a total of 21 days)	35.5 (± 4.5%)
CSCs^{HYP} exposed to INTR.20 shots	39.8 (± 5.2%)
CSCs^{HYP} exposed to CONT.5 shots	51.6 (± 6.1%)
CSCs^{HYP} exposed to INTR.40 shots	0.3 (± 0.01%)
CSCs^{HYP} exposed to CONT.15 shots	0.5 (± 0.05%)

The IC50 values (uM) of doxorubicin against MCF-7 parental, CSCs[NOR] mammospheres and CSCs[HYP] of different hypoxic shots after 72 hours treatment.

Cell Subpopulation	IC50 (uM) ± STD	Fold Change Compared to sorted normoxic Mammosphere (Control)	Fold Change Compared to Parental MCF-7
MCF-7 Parental	0.46 (±0.06)	N/A†	N/A$^\blacktriangledown$
CSCs^{NOR} mammospheres (Control)	1.90 (±0.35)	N/A$^\blacktriangledown$	4.08 ↑
CSCs^{HYP} exposed to INTR.10	4.64 (±0.15)	2.45 ↑	10.00 ↑
CSCs^{HYP} exposed to INTR.20	6.2 (±0.29)	3.28 ↑	13.39 ↑
CSCs^{HYP} exposed to INTR.30	4.101 (±0.22)	2.16 ↑	8.84 ↑
CSCs^{HYP} exposed to INTR.40	0.334 (±0.02)	0.18 ↓	0.72 ↓
CSCs^{HYP} exposed to CONT.5	7.124 (±0.19)	3.76 ↑	15.35 ↑
CSCs^{HYP} exposed to CONT.10	4.486 (±0.11)	2.36 ↑	9.67 ↑
CSCs^{HYP} exposed to CONT.15	0.441 (±0.04)	0.23 ↓	0.95 ↓

All data are expressed by means ± SD.; P<0.0001 compared to the parental group.

$^\blacktriangledown$ N/A: Value not calculated; not applicable to compare the reference to its value

† N/A: Value not calculated because we refer and compare the IC$_{50}$ of sorted CSCs^{NOR} mammospheres to MCF-7 Parental cells IC$_{50}$ not the contrary

(N/A: Not applicable, STD: Standard Deviation, uM: microMolar, ↑: Increased, ↓: Decrease)